Petroleum generation potentials and kinetics of coaly source rocks in the Kuqa Depression of Tarim Basin, northwest China

Article *in* Organic Geochemistry · April 2019

DOI: 10.1016/j.orggeochem.2019.04.007

CITATION
1

READS
134

12 authors, including:

Changchun Pan
Chinese Academy of Sciences
41 PUBLICATIONS **768** CITATIONS
SEE PROFILE

Shuang Yu
Chinese Academy of Sciences
13 PUBLICATIONS **136** CITATIONS
SEE PROFILE

Hao Xu
Chinese Academy of Sciences
5 PUBLICATIONS **21** CITATIONS
SEE PROFILE

Chengsheng Chen
Chinese Academy of Sciences
11 PUBLICATIONS **16** CITATIONS
SEE PROFILE

Organic Geochemistry 133 (2019) 32–52

Contents lists available at ScienceDirect

Organic Geochemistry

journal homepage: www.elsevier.com/locate/orggeochem

Petroleum generation potentials and kinetics of coaly source rocks in the Kuqa Depression of Tarim Basin, northwest China

Wenkui Huang [a,b], Lifei Zeng [a,b], Changchun Pan [a,*], Zhongyiao Xiao [c], Haizu Zhang [c], Zhibin Huang [c], Qing Zhao [c], Shuang Yu [a], Hao Xu [d,e], Chengsheng Chen [a,b], Dayong Liu [a], Jinzhong Liu [a]

[a] State Key Laboratory of Organic Geochemistry, Guangzhou Institute of Geochemistry, Chinese Academy of Sciences, Wushan, Guangzhou 510640, China
[b] University of Chinese Academy of Sciences, Beijing 100049, China
[c] Research and Development Research Institute, Tarim Oilfield Company, PetroChina, Korla, Xinjiang 841000, China
[d] School of Environment and Energy, South China University of Technology, Guangzhou 510006, China
[e] Dongguan Environmental Monitoring Centre Station, Dongguan 523000, China

ARTICLE INFO

Article history:
Received 4 January 2019
Received in revised form 19 April 2019
Accepted 23 April 2019
Available online 25 April 2019

Keywords:
Confined pyrolysis
Kinetic parameters
Coaly source rocks
Kuqa Depression
Tarim Basin

ABSTRACT

Confined pyrolysis experiments (gold capsules) were performed to determine the yields and kinetic features for petroleum formation for seven coal samples with hydrogen index (HI) ranging from 57 to 278 mg HC/g TOC and maturities of 0.58–0.74 %Ro from coal pits within Triassic–Jurassic strata in the Kuqa Depression, China. Gases and liquid yields were measured at regular intervals as the sealed tubes were heated at 2 and 20 °C/h and total thermal stress calculated as a vitrinte reflectance equivalent (% Re) using Easy%Ro. The total confined pyrolysate yields of oil and gaseous hydrocarbons at 1.19–1.50 % Re only account for a portion (38–53%) of the releasable moieties in measured by Rock-Eval (open) pyrolysis, suggesting that a substantial portion of (47–62%) of these moieties was rearranged and incorporated into polyaromatic residual solids. At maturities >1.87 %Re, the solid residues of the seven coals have very similar gas generative potentials (ΣC_{1-5}), which are substantially higher than their quality index (QI = (S1 + S2)/TOC) with differences ranging from 20 to 40 mg/g TOC. This result can be mainly ascribed to the differences both in methane formation mechanisms and final thermal stress levels between open (2.25 %Re) and confined pyrolysis (4.44 %Re). Only a minor portion of gaseous hydrocarbons (~32% and 44% for the Jurassic and Triassic coals, respectively) was generated up to 2.19 %Re while the major portion was generated at higher maturities. Under a heating rate of 5 °C/My, the Jurassic and Triassic coals are modeled to become effective gas source rocks with gas yield (ΣC_{1-5}) > 20 mg/g TOC at maturities of >1.76 %Re and 1.59 %Re, respectively. The abundant gaseous hydrocarbons found in the Kuqa Depression can be mainly ascribed to the high maturities of coal source rocks (>2.0 %Ro), in combination with excellent seal of thick salt and gypsum for the gas reservoirs.

1. Introduction

The Kuqa Depression in the northern Tarim Basin is a major gas-producing province of China. A number of large (giant) and medium gas fields have been found in this depression with total in-place gas reserves over 1×10^{12} m^3 (Wang, 2014). Gaseous hydrocarbons in these reservoirs are mainly derived from coaly source rocks within the Triassic–Jurassic strata (e.g., Liang et al., 2003; Zhao et al., 2005). These source rocks are currently at high maturities, mainly with maturities >1.5 %Ro but up to 2.50 %Ro or even higher (Liang et al., 2003; Zhao et al., 2005).

How to properly evaluate the petroleum generation potentials for coaly source rocks remains unresolved. Van Krevelen (1961) presented a plot of H/C vs O/C atomic ratios and demonstrated the different trends of these two ratios between natural maturation that eliminates oxygen primarily as water and CO_2, and laboratory experiments that generate more aromatic and oxygen-containing tars and incorporate additional oxygen by cross-linking reactions in the char. Peters (1986) suggested that the generative potential of liquid hydrocarbons from coals is commonly overestimated by Rock-Eval pyrolysis and is best determined by elemental analysis and organic petrography. Hunt (1991) suggested the coals that have H/C atomic ratio >0.9, Rock-Eval hydrogen indices (HI) >200 mg HC/g TOC and liptinite contents >15% are capable of generating oil.

* Corresponding author.
E-mail address: cpan@gig.ac.cn (C. Pan).

https://doi.org/10.1016/j.orggeochem.2019.04.007
0146-6380/

A series of studies demonstrated that the concentration of C_{8+} aliphatic groups determined by pyrolysis gas chromatography (py-GC) is a useful indicator of oil generative potential for coals and terrigenous organic matter (e.g., Larter et al., 1977; Smith et al., 1987; Horsfield, 1989; Curry et al., 1994, 1995; Curry, 1995; Isaksen et al., 1998). Isaksen et al. (1998) demonstrated that a typical coal from the Middle Jurassic Sleipner Formation in the North Sea with higher HI (415 mg HC/g TOC) and similar liptinite content (10%) has a substantially lower concentration of C_{15+} aliphatic groups compared with a coal from the Eocene of the Taranaki Basin, New Zealand having lower HI (362 mg HC/g TOC) and similar liptinite content (10%). The New Zealand coal is capable of generating non-volatile oil expelled as an oil phase while the North Sea coal is capable of generating only gas and volatile oil expelled as a gas phase (Isaksen et al., 1998).

Therefore, some previous studies have suggested that bulk parameters, such as H/C atomic ratio, HI value and maceral composition within a certain range are frequently not effective indicators of the oil generative potential of coals and terrigenous organic matter (Powell and Boreham, 1991; Curry et al., 1994; Isaksen et al., 1998; Killops et al., 1998). This phenomenon can be mainly ascribed to the observation that the components generated from humic coals are dominated by aromatic and phenolic hydrocarbons in open pyrolysis experiments, such as py-GC and Rock-Eval analysis, but they are mainly alkanes in closed pyrolysis experiments or in natural systems (e.g., Van Krevelen, 1961; Monthioux et al., 1985, 1986; Peters, 1986; Katz et al., 1991; Isaksen et al., 1998; Li et al., 2013; Xu et al., 2017).

The oil and gas generation process and mechanism appear to be much more complicated in gas-prone kerogen compared to oil-prone kerogen. Boreham et al. (1999) suggested that the generation of volatile hydrocarbons appears to be accompanied by a partial re-incorporation of the free hydrocarbons and bitumen into kerogen during natural maturation of coal. Dieckmann et al. (2006) and Erdmann and Horsfield (2006) documented that the recombination reactions of liquid products released from Type III kerogen at low levels of maturation result in the formation of a thermally stable bitumen, which is the major source of methane at very high maturity, and emphasized that these recombination reactions can be only simulated in closed system pyrolysis. Li et al. (2016) demonstrated that kerogen and oil do not crack separately in the experiments of coal plus oil and suggested that the interaction between kerogen and oil components leads to the generation of hydrocarbon gases.

The precise amounts of oil and hydrocarbon gases generated from a source rock cannot be obtained from observations on natural samples (e.g., Price and Wenger, 1992). Such data can only be determined from pyrolysis experiments under conditions comparable to the natural environment. Some studies have demonstrated that the reaction medium plays an important role in source rock pyrolysis (Mansuy and Landais, 1995; Mansuy et al., 1995; Michels et al., 1995). Monthioux et al. (1985, 1986) first reported pyrolysis experiments on coals under confined system using gold capsules and demonstrated that the pyrolysates are very similar to oils in reservoirs and bitumen extracted from the coal source rocks. In a natural system, the retained oil is mainly absorbed by the kerogen in source rocks (Pepper, 1992; Sandvik et al., 1992). In confined pyrolysis experiments, the released components (hydrocarbons, polar components, and water) and kerogen in the compressed gold capsules are in close contact with each other and so the reaction medium is more comparable to a source rock in a natural system where oil expulsion leads to a lower gas yield for a source rock compared to a closed system. Xiang et al. (2016) presented an approach to predict the amount of expelled oil and the accumulative yield of gaseous hydrocarbons after oil expulsion.

Oil and gas formation from coaly source rocks is generally described using first-order parallel kinetics with a distribution of activation energies and a single frequency factor although the reaction mechanism for oil and gas formation from this type of source rocks is very complicated (e.g., Tang et al., 1996; Behar et al., 1997; Boreham et al., 1999; Dieckmann et al., 2006; Erdmann and Horsfield, 2006). Ungerer and Pelet (1987) showed that the kinetic parameters of oil and gas formation determined from laboratory pyrolysis of an immature kerogen sample apply to the conditions of sedimentary basins, although the time and temperature scale are completely different. Behar et al. (1997) demonstrated that for types I, II and II-S kerogens the kinetic parameters derived from experiments in an open system with a single frequency factor and a discrete series of activation energies are valid, while for Type III kerogen the unique frequency factor found by optimization of the Rock-Eval S2 peak may be an average between a very low value around 10^{11}–10^{12} s^{-1} for the early generation of paraffinic oil and a very high value around 10^{14}–10^{15} s^{-1} for the late generation of gas. Burnham and Braun (1999) suggested that the discrete activation-energy distribution derived by assuming a linear relationship between the logarithm of the frequency factor and the activation energy is better fitted to the result of coal pyrolysis experiments. Dieckmann (2005) determined the kinetic parameters consisting of a distribution of activation energies and a distribution of frequency factors for source rocks with different kerogen types and suggested that the prediction for the onset of petroleum formation from source rocks with Type III kerogen could be more accurate using this modified model than the conventional model with a single frequency factor.

The yields of oil and gaseous hydrocarbons and the kinetic features for oil and gas generation from the Triassic–Jurassic coals in the Kuqa Depression are not well documented in previous studies (e.g., Liang et al., 2003; Zhao et al., 2005; Jia and Li, 2008; Zhang et al., 2011; Guo et al., 2016). The purposes of this paper are to: (1) document the differences between the yields of oil and gaseous hydrocarbons in confined pyrolysis experiments (closed system) and generative potentials in Rock-Eval analysis (open system) from these coals, and (2) determine the kinetic parameters for oil and gas generations based on yield data from confined pyrolysis for modeling oil and gas generation from coal source rocks in this depression.

2. Geological setting

The Kuqa Depression is located in the northern part of the Tarim Basin, south of the Tianshan Mountains, NW China (Fig. 1). It can be further divided into four structural belts (slope) and three sags: the Northern monoclinal belt, the Kelasu-Yiqikelike structural belt, the Qiulitage structural belt and the Southern gentle slope from north to south, and the Wushi, Baicheng and Yangxia sags from west to east (Fig. 1; Lei et al., 2007; Jia and Li, 2008; Guo et al., 2016). This depression has experienced three tectonic stages: (1) a foreland basin from the Late Permian to the Middle Triassic, (2) an extensional rift basin from the Late Triassic to the Middle Jurassic, and (3) a rejuvenated foreland basin from the Cretaceous to Quaternary (Graham et al., 1993; Jia et al., 2000, 2002; Liang et al., 2003; Zhao et al., 2005; Zhang et al., 2011; Guo et al., 2016).

At the extensional rift stage from the Late Triassic to Middle Jurassic, lacustrine and marginal lacustrine–swamp transitional sediments were deposited in the Kuqa Depression with a total thickness of over 1000 m in relatively warm and humid climates (Fig. 2; Jia et al., 1995; Jia and Li, 2008). During the Early Cretaceous, the Kuqa foreland basin evolved into a shallow lake with a relatively arid climate (Yang et al., 2005). Coarse clastic rocks of alluvial fan, fan delta and braided river facies sediments formed

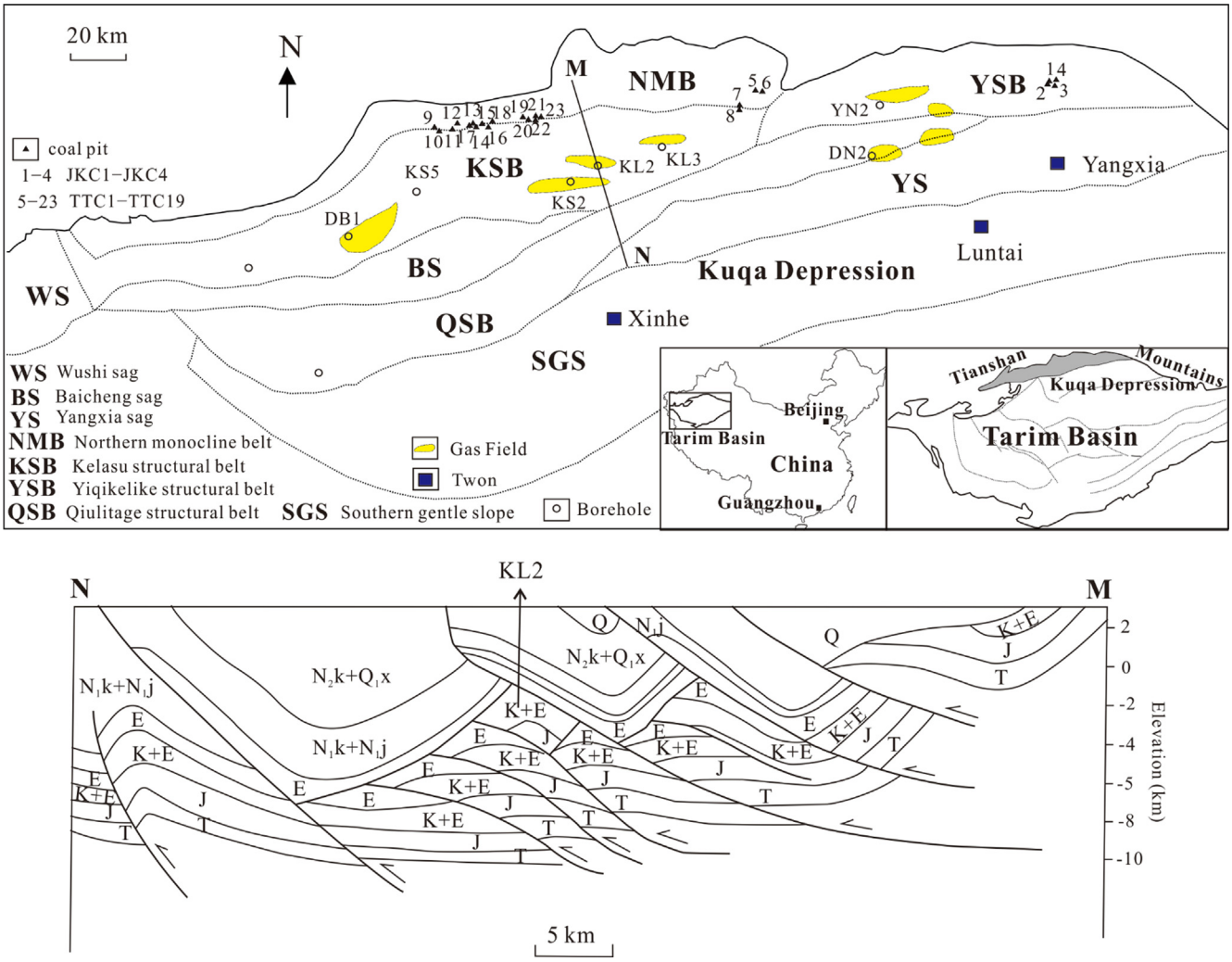

Fig. 1. Location map of the Kuqa Depression and sample locations (modified from Jia and Li, 2008).

in the mountain front in the north. The lake was wide but shallow, with gentle slopes. The river mouths were frequently blocked with sediments so that rivers changed their channels repeatedly. As a result, deltas were often connected laterally, shaping a delta apron in the mountain front (Jia and Li, 2008). During the Late Cretaceous, regional uplift began in the Kuqa region. The Yiqikelike and Tugerming anticlines started to form under horizontal compressions. At the end of Paleogene, the northern Tarim Basin was uplifted to form the Tianshan Mountain belts. The rapid rise of the Tianshan Mountains led to the accumulation of thick reddish continental sediments in the Kuqa Depression. From the Miocene onwards strong compression and thrusting led to the formation of a series of thrust belts from north to south and various fault-related folds. Clastic sediments derived from the north were deposited in the rejuvenated foreland basin. The bottom slippage uplifted from north to south, leading to a series of typical north-south oriented thrust structures (Fig. 1; Zhao et al., 2005; Jia and Li, 2008; Zhang et al., 2011).

Six source rocks have been identified within the Middle Triassic to Middle Jurassic strata in the Kuqa Depression: the Middle–Upper Triassic Kelamayi Formation ($T_{2-3}k$), the Upper Triassic Huangshanjie (T_3h) and Taliqike formations (T_3t), the Lower Jurassic Yangxia Formation (J_1y), and the Middle Jurassic Kezilenuer (J_2k) and Qiakemake formations (J_2q; Liang et al., 2003; Zhao et al., 2005). The Kelamayi ($T_{2-3}k_3$) and Huangshanjie formations (T_3h) contain lacustrine mudstone source rocks with mainly Type III kerogen. The Qiakemake Formation (J_2q) contains lacustrine mudstone source rocks but with mainly Type II kerogen. The Taliqike (T_3t), Yangxia (J_1y) and Kezilenuer (J_2k) formations all contain coaly source rocks (Liang et al., 2003; Zhao et al., 2005). Potential reservoir rocks include: the sandstone units in the Triassic Ehuobulake (T_1oh), Kelamayi ($T_{2-3}k_3$), Jurassic Ahe (J_1a), Yangxia (J_1y), Kezilenuer (J_2k), Cretaceous Baxigai (K_1b), Bashijiqike (K_1bs), Paleogene Kumugeliemu ($E_{1-2}km$), Neogene Jidike (N_1j), and Kangcun (N_1k) formations. The salt and gypsum unit within the Kumugeliemu Formation ($E_{1-2}km$) forms an excellent regional seal for the preservation of the hydrocarbons in the Cretaceous and Paleogene reservoirs (Fig. 2).

In the Kuqa Depression, the total thickness of coal beds averages about 12 m within the Kezilenuer Formation (J_2k) and 24 m within the Taliqike Formation (T_3t; Cui 2011; Yu et al., 2013; An et al., 2016). Coal beds within the Yangxia Formation (J_1y) have roughly the same total thickness as those within the Kezilenuer Formation (J_2k) and the total thickness of coal beds within these two formations averages 20–30 m (Jia and Li, 2008). Therefore, coal beds potentially provided the major gas components for gas fields in the Kuqa depression (Liang et al., 2003; Jia and Li, 2008).

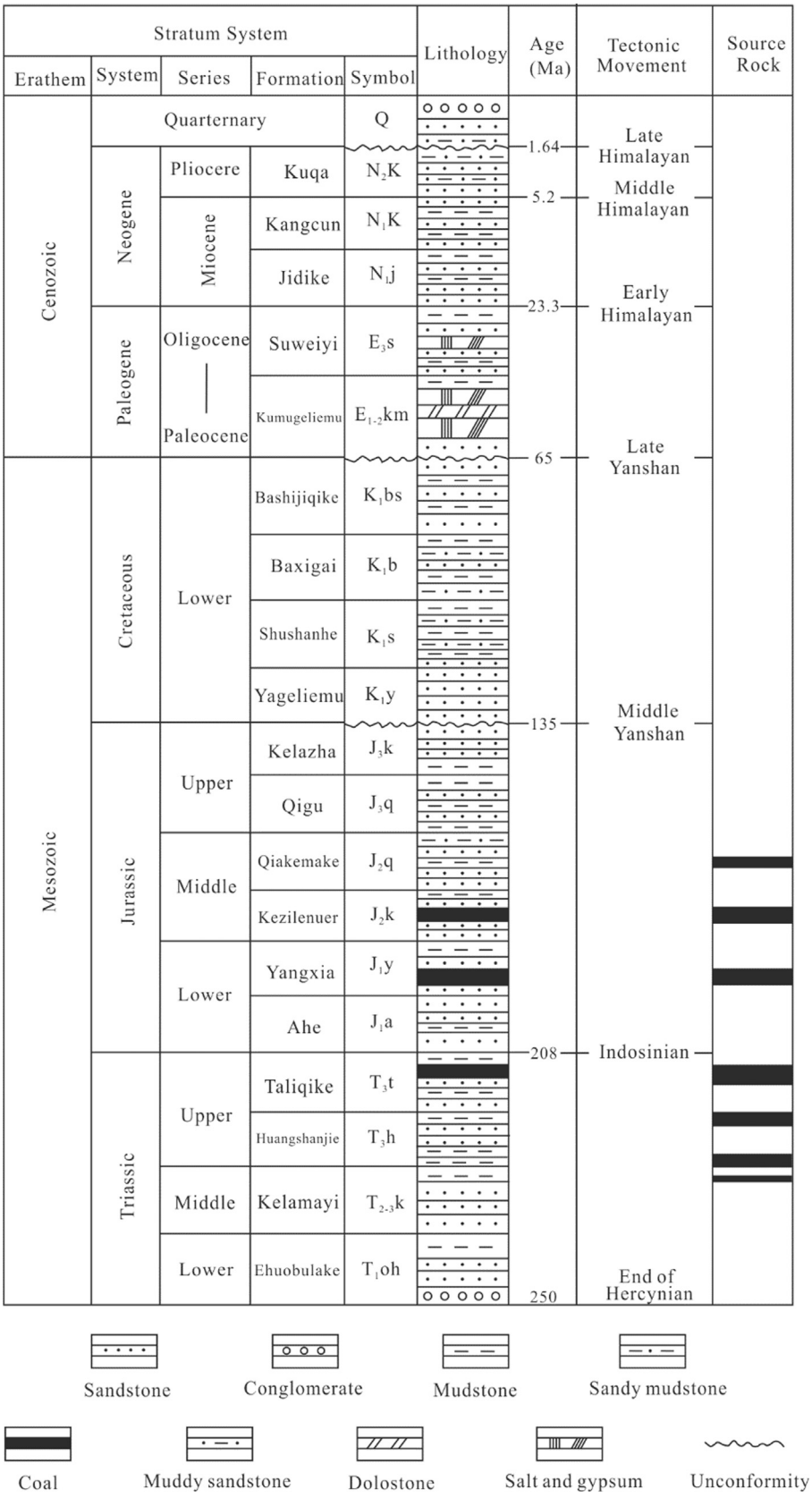

Fig. 2. Mesozoic–Cenozoic Stratigraphy of the Kuqa Depression (modified from Guo et al., 2016).

3. Experimental

3.1. Samples

Previous studies have demonstrated that, for the Triassic–Jurassic terrigenous source rocks in the Kuqa depression, the outcrop samples are heavily weathered with substantially lower hydrogen index (HI < 100 mg HC/g TOC) while core samples from boreholes have high maturities (>0.90 %Ro; Liang et al., 2003; Zhao et al., 2005). In the present study, coals from coal pits were used for pyrolysis experiments to determine the yields and kinetic parameters for oil and gas generations from samples that are less weathered and of lower maturity.

Twenty-three coal samples were collected from coal pits, including four coals from coal beds within the Middle Jurassic Kezilenuer Formation (J_2k) and 19 coals within the Upper Triassic Taliqike Formation (T_3t, Fig. 1). All coals were first cleaned using distilled or de-ionized water and then ground into powder (about 200 mesh). A small aliquot of powder was taken from each sample for measurement of total organic carbon content (TOC) using a Leco-230C/S analyzer. Another small aliquot of powder was taken for Rock-Eval analysis using an IFP Rock-Eval 6. For the measurement of vitrinite reflectance (%Ro), polished sections for all coals were prepared on coal lumps. Definitions for the measured and calculated parameters for coals and products of pyrolysis experiments are listed in the Appendix A. The analytic results for the 23 coals are shown in Table 1 and Fig. 3.

Four coals from JKC1 to JKC4 within the Kezilenuer Formation (J_2k) have TOC, HI, Tmax and %Ro values in the range 66.3–74.4%, 57–183 mg HC/g TOC, 424–437 °C and 0.58–0.66, respectively. The nineteen coals from TTC1 to TTC19 within the Taliqike Formation (T_3t), have TOC, HI, Tmax and %Ro values in the range 55.3–82.9%, 58–302 mg HC/g TOC, 433–496 °C and 0.58–0.96, respectively (Table 1, Fig. 3). Twelve of the nineteen coals with relatively lower maturities (Tmax 433–458 °C, 0.58–0.84 %Ro) have HI values >200 mg HC/g TOC while the other seven with relatively higher maturities (Tmax 436–496 °C, 0.64–0.96 %Ro) have HI values ranging from 58 to 170 mg HC/g TOC. It appears that the Taliqike Formation (T_3t) coals have relatively higher HI values than those within the Kezilenuer Formation (J_2k, Fig. 3). Seven coals, i.e. JKC1, JKC2, JKC3, TTC1, TTC4, TTC11 and TTC18, were selected for pyrolysis experiments to determine the yields and kinetic parameters for oil and gas generation.

3.2. Confined pyrolysis experiments

The approach for confined pyrolysis experiments on the seven coals is similar to that described in our previous studies (Pan et al., 2008, 2010, 2012; Li et al., 2013; Xiang et al., 2016). Briefly, gold capsules containing a weighed amount of coal powder without extraction (20–90 mg) were placed in steel pressure vessels. The internal pressure of the vessels, connected to each other with tubing, was maintained at 50 MPa by pumping water into or out of the vessels during the experiments. The error of the pressure is <±0.1 MPa. The vessels were heated in an oven from room temperature to 250 °C over 10 h, and then from 250 °C to 600 °C at a rate of 2 °C/h or 20 °C/h. Two thermocouples were used to measure the temperature of the pyrolysis experiments and to check each other. The error of the recorded temperatures is <±1 °C. Vessels containing gold capsules were removed from the oven at temperature intervals of 12 °C or 24 °C from 333.1 °C to 598.9 °C at 20 °C/h and from 322.4 to 599.7 °C at 2 °C/h.

3.3. Analysis of gas components

After pyrolysis, the volatile components in the capsules were collected in a special sampling device connected to an Agilent 6890 N GC modified by Wasson ECE Instrumentation, as described previously (Pan et al., 2006, 2008; Li et al., 2013; Xiang et al., 2016). Briefly, the device was first evacuated to $<1 \times 10^{-2}$ Pa at room temperature (25 °C). The gold capsule was then pierced with a needle under vacuum, allowing the gases to escape into the device. The valve connecting the device and the modified GC was open to allow the gas to enter the GC, through which the GC analyses of both the organic and inorganic gas components were performed in an automatically controlled procedure. The oven temperature for the hydrocarbon gas analysis was initially held at 70 °C for 6 min, ramped from 70 to 130 °C at 15 °C/min, from 130 to 180 °C at 25 °C/min, and then held at 180 °C for 4 min, whereas it was held at 90 °C for the inorganic gas analysis. The analysis of all gases

Table 1
Total organic carbon content (TOC) and Rock-Eval parameters of pit coals.

	Strata	TOC %	S1	S2	S3	HI	OI	Tmax	%Ro
JKC1	J_2k	71.9	2.9	101.1	11.4	141	16	424	0.58
JKC2	J_2k	74.4	4.5	136.2	3.3	183	4	437	0.66
JKC3	J_2k	72.8	0.3	41.6	5.5	57	8	433	0.62
JKC4	J_2k	66.3	0.5	66.6	5.8	101	9	426	0.61
TTC1	T_3t	75.3	4.2	208.1	4.1	276	5	433	0.73
TTC2	T_3t	75.9	7.3	190.1	2.2	250	3	439	0.74
TTC3	T_3t	77.0	5.7	155.9	2.5	203	3	436	0.72
TTC4	T_3t	77.3	4.8	172.0	1.8	223	2	447	0.74
TTC5	T_3t	76.2	11.7	230.4	4.8	302	6	439	0.71
TTC6	T_3t	79.7	0.5	103.5	1.1	130	1	485	0.96
TTC7	T_3t	81.6	0.6	47.3	3.2	58	4	496	0.82
TTC8	T_3t	62.6	2.8	105.3	1.4	168	2	472	0.84
TTC9	T_3t	71.2	1.1	70.5	0.9	99	1	495	0.88
TTC10	T_3t	77.8	8.5	180.8	1.8	233	2	444	0.69
TTC11	T_3t	70.5	4.2	196.4	3.4	278	5	437	0.58
TTC12	T_3t	75.0	5.9	218.7	2.8	292	4	438	0.64
TTC13	T_3t	65.3	2.4	69.6	2.3	107	3	447	0.74
TTC14	T_3t	55.3	2.1	93.8	9.2	170	17	436	0.64
TTC15	T_3t	57.5	4.9	115.9	3.5	202	6	458	0.73
TTC16	T_3t	80. 7	7.0	167.5	1.2	208	2	457	0.84
TTC17	T_3t	82.9	8.7	138.6	1.2	167	1	468	0.85
TTC18	T_3t	79.3	9.6	200.4	6.5	253	8	458	0.74
TTC19	T_3t	82.1	6.2	172.2	3.7	210	4	458	0.71

S1 and S2: in "mg HC/g rock"; S3: in "mg CO_2/g rock"; HI: in "mg HC/g TOC"; OI: in "mg CO_2/g TOC"; Tmax is in "°C".

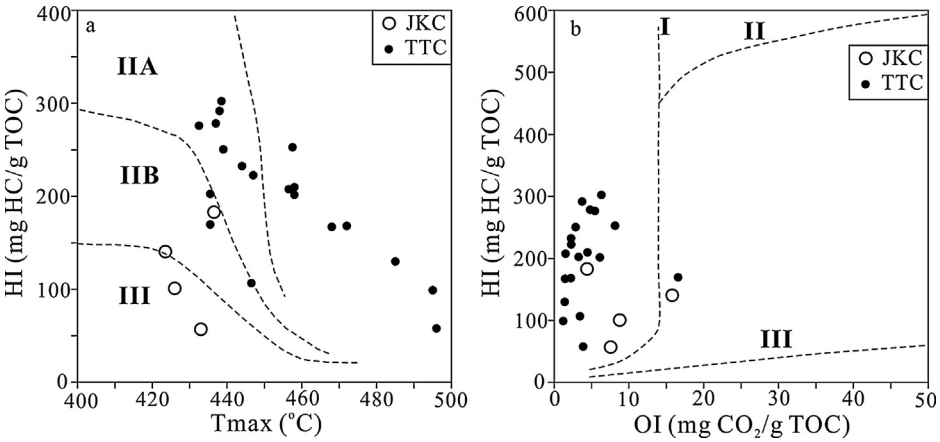

Fig. 3. Crossplots of HI vs Tmax (a) and HI vs OI (b) from Rock–Eval analyses of pit coals within the Middle Jurassic Kezilenuer Formation (J_2k, JKC) and Upper Triassic Taliqike Formation (T_3t, TTC).

was carried out by one single injection. A test with external standard gases indicated that the amounts of gas products measured using this device had better than 0.5% relative error.

3.4. Analyses for bitumen and liquid components (ΣC_{8+})

The method for the analysis of liquid components (ΣC_{8+}) is similar to that described in previous studies (Pan et al., 2009; Li et al., 2013; Xiang et al., 2016). After analysis for gas components, the capsules that were heated at lower temperatures (322–490 °C) were cut swiftly into several pieces in a vial, which contained about 3 ml pentane. Two internal standards of deuterated *n*-C_{22} and *n*-C_{24} *n*-alkanes were then added to each vial with amounts ranging from 0.010 to 0.015 mg. Following five ultrasonic treatments of 5 min per treatment, these vials were allowed to settle for 72 h until the pentane solutions became clear. The pentane solutions in all vials were directly injected into a HP6890 GC fitted with a 30 m × 0.32 mm i.d. column coated with a 0.25 μm film of HP-5, employing nitrogen as carrier gas. The oven temperature was programmed as follows: 50 °C for 5 min, raised from 50 °C to 150 °C at 2 °C/min, and from 150 °C to 290 °C at 4 °C/min, and then held at 290 °C for 15 min.

Eighteen non-biodegraded light oils from boreholes in the northwestern and central areas of the Junggar Basin were analyzed using the same method. The amounts of total liquid components (ΣC_{8+}) in the 18 oil samples were in the range 425–715 mg/g oil with an average of 563 mg/g. The amount of total liquid components (ΣC_{8+}) for each capsule of the seven coals was divided by 0.563, the averaged value for the eighteen oils (563 mg/g oil), yielding the amount of oil (S_O) produced during pyrolysis for each capsule. The oil yield that is converted from the yield of total liquid components (ΣC_{8+}) can be considered the yield of a normalized oil, which is comparable to oils in reservoirs, containing 56.3% detectable components by GC-FID, the remaining 43.7% represented non-volatile polar components (asphaltene and resin) and unresolved complex mixtures (UCM) in chromatograms.

After GC analyses, the samples in these vials were filtered to separate the pentane solution and the residual solid. The residual solids were Soxhlet extracted with dichloromethane:methanol (93:7, v/v) for 72 h. The extracts were combined with the initial pentane soluble fraction to obtain the heavy pyrolysates (bitumen) and quantified by gravimetric method.

After Soxhlet extraction for bitumen, the residual solids were recovered from the capsules heated from 322 to 479 °C at 2 °C/h and TOC and Rock-Eval analyses were performed as described earlier.

4. Results and discussion

4.1. Mass balance

For the six coals JKC1, JKC2, TTC1, TTC4, TTC11 and TTC18, the liquid components generated in confined pyrolysis experiments at temperatures of 322–419 °C contain mainly *n*-alkanes, comparable to the non-biodegraded natural oils (Figs. 4 and 5). At this temperature range, the heated coals reached thermal stress levels in the range 0.66–1.50 %Re (vitrinite reflectance equivalent from Easy%Ro; Sweeney and Burnham, 1990) spanning the oil generative window. Therefore, oil yields (S_O) obtained under these confined pyrolysis condition can be considered to be similar to those in the natural system. However, coal JKC3 generates mainly aromatic components under confined pyrolysis within the oil generative window, strikingly different from the other six coals (Fig. 5c). As a result, the measured yields of liquid components (ΣC_{8+}) within the oil window for coal JKC3, are substantially higher (4.6–42.2 mg/g TOC) than those for coals JKC1 and JKC2 (6.9–19.9 and 3.3–22.4 mg/g TOC, respectively, although coal JKC3 has lower initial QI (quality index = (S1 + S2)/TOC) of 57.5 mg HC/TOC than coals JKC1 (144.6 mg HC/g TOC) and JKC2 (189.0 mg HC/g TOC). Isaksen et al. (1998) suggested that the main control on the oil potential of humic coals is the concentration of long-chain aliphatic hydrocarbons in the coal matrix. Here, we present an alternative approach for coal JKC3 to estimate oil yields (S_O) based on the yield of total *n*-alkanes (Σn-C_{8+}) from the confined experiments, which could be comparable to those in natural system. The averaged ratios of the yield of total *n*-alkanes to oil yield (Σn-C_{8+}/S_O) for the other six coals are in the range 0.118–0.150 (and hence within the oil generative window) at temperatures of 322–419 °C. Oil yields (S_O) for coal JKC3 were obtained using the yields of total *n*-alkanes from this coal and the averaged Σn-C_{8+}/S_O ratios of the other six coals at similar temperatures. The amounts of oil (S_O) and gaseous hydrocarbons (ΣC_{1-5}) for the seven coals heated from 322 to 479 °C at 2 °C/h are shown in Fig. 6. The yields of gaseous hydrocarbons (ΣC_{1-5}) increase consistently while the oil yields (S_O) first increase with temperature to maximum values at about 394 °C with 1.19 %Re, and then decrease for all seven coals (Fig. 6).

The Rock-Eval parameter S1 + S2 is defined as the generative potential for 1 g of a source rock (mg HC/g Rock; Espitalié et al., 1977). Pepper and Corvi (1995a) defined a quality index (QI = (S1 + S2)/TOC) as the generative potential for 1 g of total organic carbon (mg HC/g TOC) in the source rock. In the present pyrolysis experiments, we used the powder of the initial coals without extraction because bitumen is an important precursor

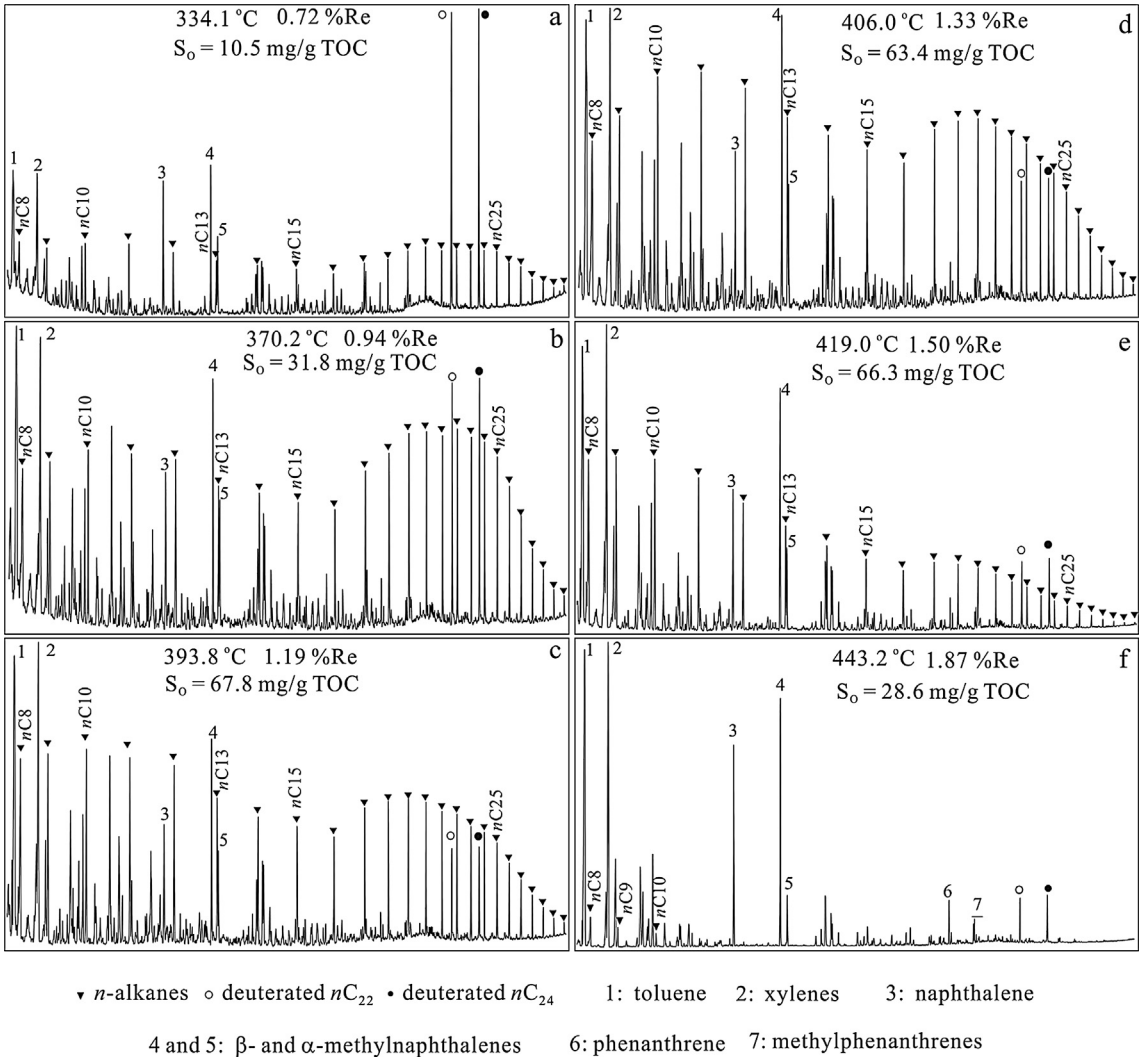

Fig. 4. Selected gas chromatograms of liquid hydrocarbons at 334.1, 370.2, 393.8, 406.0, 419.0 and 443.2 °C for coal TTC11 at a heating rate of 2 °C/h.

for oil and gas generation from the initial coal. For capsules heated from 322 to 480 °C at a heating rate of 2 °C/h, the residual solid was recovered and analyzed for TOC by Leco-230C/S and Rock-Eval (Fig. 6). After heating, organic carbon in the initial coal is distributed as oil, gaseous hydrocarbons, CO_2 and residual solid. Defining the yields of CO_2 and total oil and gaseous hydrocarbons as S_{CO2} and S_{OG}, respectively and assuming that the carbon content in the total oil and gaseous hydrocarbon is 80%, for the initial coal with 1 g of total organic carbon, the amounts of organic carbon in the forms of CO_2, total oil and gaseous hydrocarbons and residual solid would be $S_{CO2} \times 12/44$, $0.8 \times S_{OG}$, and $1000 - 0.8 \times S_{OG} - S_{CO2} \times 12/44$ mg, respectively. We define QIR as the difference of the generative potential between the initial coal with 1 g of organic carbon and the corresponding residual solid after heating. QIR can be calculated by formula (1):

$$QIR = QIi - (1000 - 0.8 \times S_{OG} - S_{CO2} \times 12/44) \times QIh/1000 \quad (1)$$

Here, QIi and QIh are the QI values for the initial coal prior to heating and residual solid after heating, respectively.

In principle, QIR would be equal to S_{OG}, the total yield of oil plus gaseous hydrocarbons (ΣC_{1-5}) after heating. However, S_{OG} is substantially lower than the QIR values for all seven coals (Fig. 6). For these samples, S_{OG} in confined pyrolysis experiments is considered to be similar to those in the natural system. In contrast, oil generative potentials for humic coals are commonly overestimated by Rock-Eval parameter QI or HI because the released components during Rock-Eval pyrolysis contain high proportion of aromatic hydrocarbons and phenols (e.g., Peters, 1986; Katz, et al., 1991; Isaksen et al., 1998). For example, the compositions of pyrolysates as characterized by open system pyrolysis-GC from humic coals with HI around 200 mg HC/g TOC in an open system (Rock-Eval type), are dominantly by aromatic components and polars, especially phenols (Katz et al., 1991). Isaksen et al. (1998) reported similar results for pyrolysis-GC chromatograms of humic coals from the Sleipner Formation with HI ranging from 220 to 415 mg/g TOC. In the present study, the difference between parameters QIR and the measured S_{OG} can be mainly ascribed to the compositional difference of pyrolysates between confined pyrolysis and Rock-Eval pyrolysis. This difference can be interpreted as follows:

(1) Previous studies have documented that the released liquid components can be incorporated into solid kerogen in closed pyrolysis and natural systems (McNeil and BeMent, 1996; Boreham et al., 1999; Dieckmann et al., 2006; Erdmann and Horsfield, 2006; Pan et al., 2012; Li et al., 2013, 2016; Burnham and Braun, 2017). Aromatic components and phenols are likely preferentially incorporated in the residual solid (Burnham and Braun, 2017). In contrast, pyrolysates

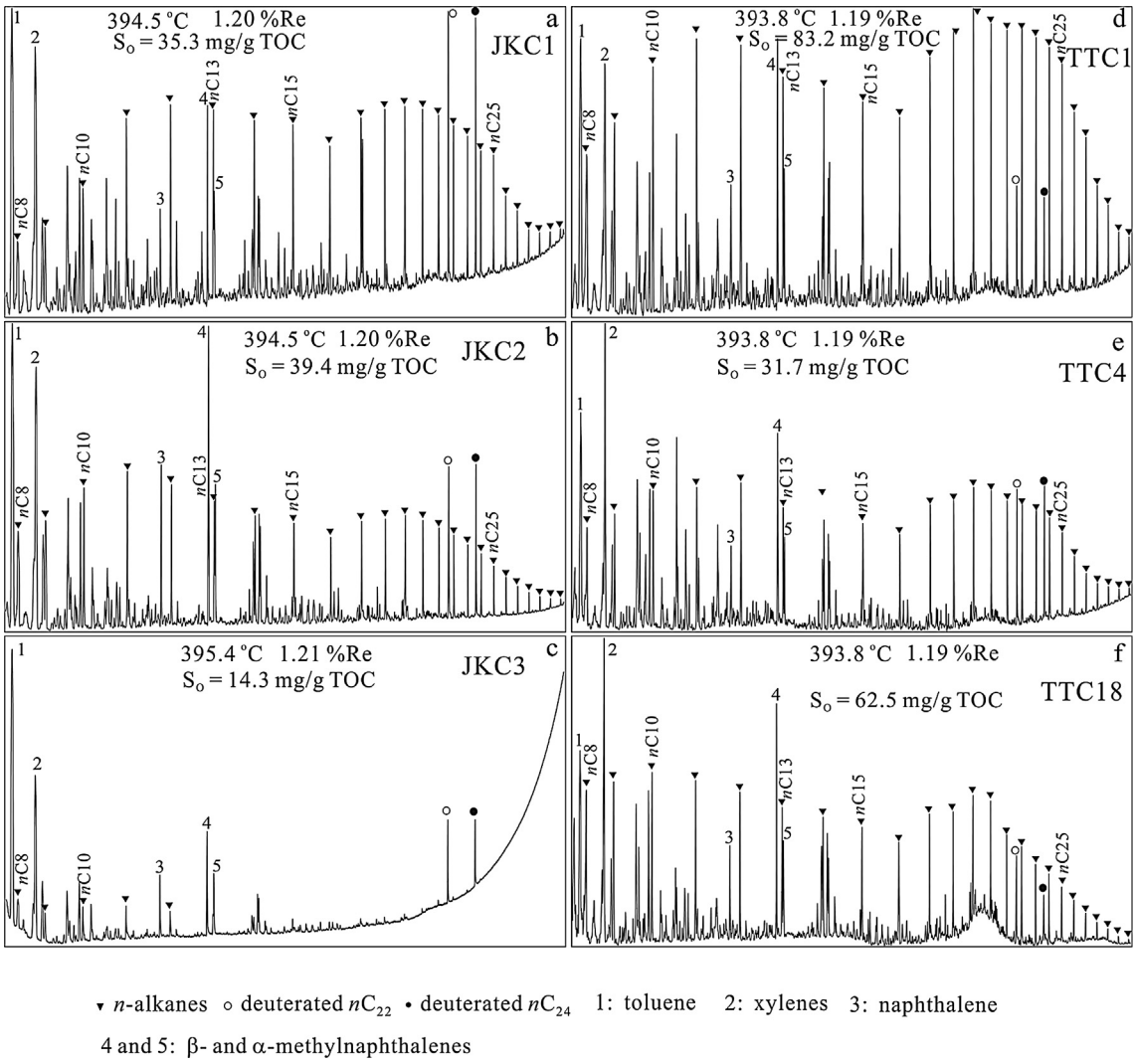

Fig. 5. Selected gas chromatograms of liquid hydrocarbons at about 394 °C for coals JKC1, JKC2, JKC3, TTC1, TTC4 and TTC18 at a heating rate of 2 °C/h.

are removed quickly from the reaction system once they are released in an open system. As a result, pyrolysates from humic coals contain much higher amounts of aromatic components and phenols in an open system than in a closed system.

(2) Open pyrolysis (Rock-Eval type) is routinely performed at a heating rate of 25 °C/min, substantially higher than in the confined system in the present study, i.e., 2 °C/h and 20 °C/h. Therefore, pyrolysis temperatures are higher in an open system than in a confined system at an equivalent maturity level. Humic coals possibly release higher amounts of aromatic components and phenols at higher temperatures than at lower temperatures (Zieger et al., 2018).

(3) In a closed system, chemical interactions among released components and between the released components and residual solid are very complex, including net hydrogen disproportionation reactions that result in the formation of hydrogen-rich oil and gas components and insoluble, hydrogen-poor solid residue. Oxygen disproportionation reactions promote the formation of CO_2, retard the formation of phenols and decrease the O/C ratio in residual solid. The overall result is that components generated from humic coals are more chemically stable and less reactive in a closed system than in an open system (Smith et al., 1989; Boudou et al., 1994; Burnham et al., 1995; Mansuy et al., 1995; Mansuy and Landais, 1995; Leif and Simoneit, 2000; Michels et al., 2000; Alexander et al., 2009, 2011).

We used the ratio QOGR (QIR/S_{OG}) to document the relationship between QI (QIh) of the residual solid after heating and S_{OG} during confined pyrolysis. Coals JKC1, JKC2, TTC1, TTC11 and TTC18 have a similar trend in QOGR variations with temperature (Figs. 6 and 7). However, for all seven coal samples, at 394–419 °C or 1.19–1.50 %Re with maximum oil yields, QOGR ranges from 1.9 to 2.6, demonstrating that a portion of the 38–53% of releasable moieties in Rock-Eval pyrolysis (QIi), mainly aliphatic compounds present in the coals prior to heating, contribute to the formation of oil and gaseous hydrocarbons (S_{OG}) while the other portion of 47–62% of these moieties (QIi), mainly aromatics and phenols, are rearranged and incorporated into polyaromatic solids.

Coal TTC4 shows different variation trends for S2, HI and QOGR compared to the other coal samples (Figs. 6e and 7). At 322.5 and 334.1 °C, parameter S2 values are even higher for the residual solid than for the initial coal prior to heating. A similar result was also reported by Burnham et al. (1995). Previous studies have reported that HI for coals increases significantly from the immature stage to the onset of oil generation (Boudou et al., 1994; Killops et al., 1998,

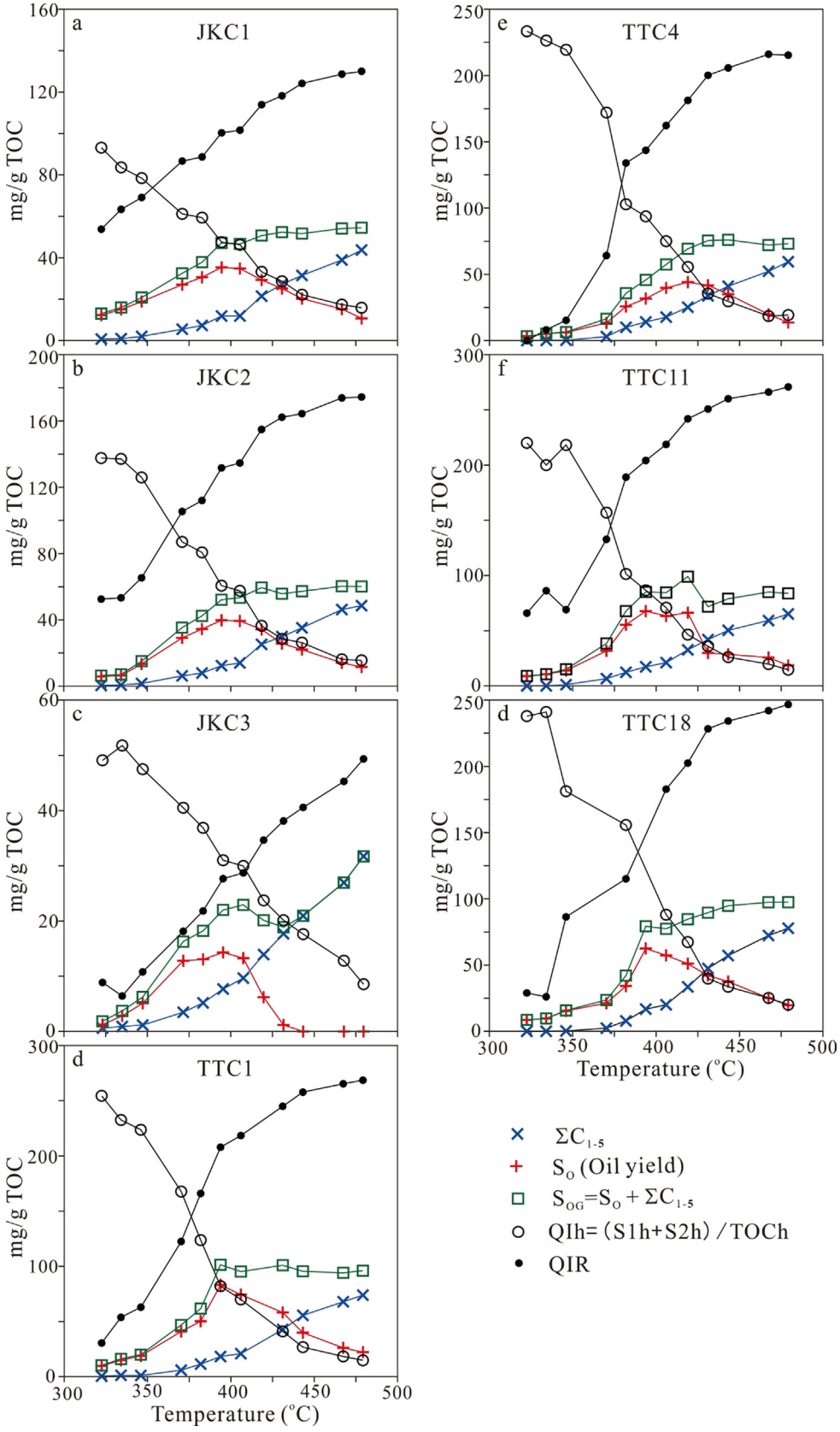

Fig. 6. QI, QIR, gas yield, oil yield and the total yield of oil plus gas for the seven coals within 322.4–478.4 °C at a heating rate of 2 °C/h. QI (quality index) = (S1 + S2)/TOC; QIR: quality index reduction value, calculated from formula (1); ΣC_{1-5}: gas yields; S_O: oil yield; S_{OC}: total yield of oil plus gas.

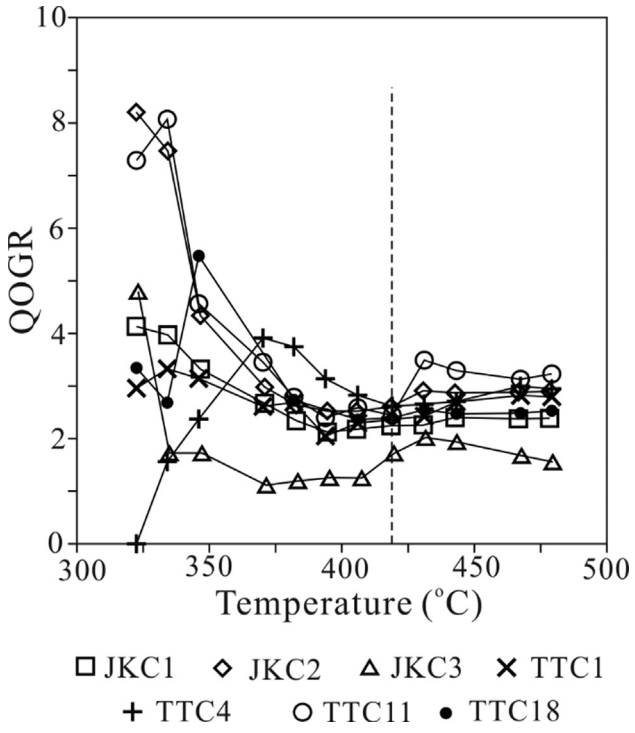

Fig. 7. QOGR values for the seven coals within 322.4–378.4 °C at a heating rate of 2 °C/h. QOGR = QIR/S_{OG}, QIR and S_{OG}, see the caption for Fig. 6.

2002; Boreham et al., 1999; Sykes and Snowdon, 2002). Boudou et al. (1994) ascribed the lower HI for coal at immature stages to oxygen-group suppression of the FID during Rock-Eval pyrolysis. Boreham et al. (1999) suggested that the incorporation of volatile components (mostly polar) into kerogen leads to an HI increase in immature stages of coal. Sykes and Snowdon (2002) suggested that the HI increase for New Zealand Late Cretaceous–Cenozoic humic coals is unlikely caused by decarboxylation leading to hydrogen concentration or by oxygen-group suppression of the FID, but can be mainly ascribed to structural rearrangement of the coal macromolecular matrix during diagenesis and catagenesis. Killops et al. (2002) also suggested that structure rearrangements may exert the primary influence on the HI increase of New Zealand coals.

In the present study, the possibility that the extra volatile components are incorporated into kerogen can be ruled out because no oil or bitumen was added to the coal samples prior to pyrolysis. After pyrolysis, the generated oil was separated from the residual solid. At 322.5 °C, the CO_2 yield (S_{CO2}) of coal TTC4 is only 0.9 mg/g TOC, lower than those of the other six coal samples, particularly the four coals JKC1, JKC2, JKC3 and TTC1. Therefore, the higher QIh value for the residual solid at 322.5 °C in comparison with the QIi value of the initial coal for coal TTC4 is unlikely caused by decarboxylation but most likely related to structure rearrangement of kerogen as suggested by Killops et al. (2002) and Sykes and Snowdon (2002). This type of structural rearrangement leads to more aromatic and phenolic moieties, as well as alkanes, releasable in Rock-Eval pyrolysis from the residual solid compared to the initial coal prior to heating for coal TTC4. For coal TTC4, we used the QIh value at 322.5 °C (233.3 mg/g TOC) as QIi for the initial coal prior to heating to calculate QIR by formula (1).

Previous studies have demonstrated that the amounts of oil generated from Type I kerogens in confined pyrolysis are similar to HI values (Xiang et al., 2016), and therefore, QOGR values are around 1.0 for these kerogens. For oil-prone kerogens, components released from open system pyrolysis are dominated by alkane-alkene pairs, similar in carbon number distribution to normal oils (e.g., Katz et al., 1991; Tegelaar and Noble, 1994).

The three Jurassic coals JKC1, JKC2 and JKC3 have initial HI values of 141, 183 and 57 mg HC/g TOC and maximum S_O values of 34.8, 39.8 and 14.3 mg/g TOC while the four Triassic coals TTC1, TTC4, TTC11 and TTC18 have initial HI in the range 223–278 mg HC/g TOC and maximum S_O in the range 44.1–83.2 mg/g TOC (Table 1). The maximum S_O values are clearly positively related to the initial HI values of the seven coals prior to heating. These seven coals have maturities of 0.58–0.74 %Ro, in the range for the maximum HI for coal samples suggested by Sykes and Snowdon (2002). Killops et al. (1998) suggested a threshold oil amount of 40 mg/g TOC is needed for oil expulsion from coal. Based on this threshold value, all three Jurassic coals are ineffective oil source rocks while all the four Triassic coals are effective oil source rocks.

4.2. Gas generation at the highly post-mature stage

At 443.2 °C at 2 °C/h (1.87 %Re) or 488.9 °C at 20 °C/h (1.95 %Re), liquid components are dominated by toluene, xylenes, naphthalene, methylnaphthalenes, phenanthrene, and methylphenanthrenes with very low amount of short chain *n*-alkanes (Fig. 4f). These components can be treated as a part of the residual solid because they generate very little gaseous hydrocarbons during cracking. At this maturity level, oil-cracking to gas has effectively been completed. Products for pyrolysis experiments at this and higher maturities consist only of gases and residual solid.

At the highly post-mature stage (>1.87 %Re), the yields of the total gaseous hydrocarbons (ΣC_{1-5}) increase at similar rates with increasing %Re for the seven coals (Fig. 8a and c) indicating that the residual solid for the seven coals have similar generative potentials for gaseous hydrocarbons (GGP) at >1.87 %Re even though these coals have substantially different initial HI values ranging from 57 to 278 mg/g TOC prior to heating. GGP values for residual solid at >1.87 %Re at 443.2 °C at 2 °C/h and >1.95 %Re at 488.9 °C at 20 °C/h can be calculated using the following formula (2):

$$GGP = (\Sigma C_{1-5}max - \Sigma C_{1-5}) \times 1000/(1000 - 0.8 \times \Sigma C_{1-5} - S_{CO2} \times 12/44) \quad (2)$$

Here, ΣC_{1-5}max is the maximum yield of total gaseous hydrocarbons (ΣC_{1-5}). We assume that ΣC_{1-5} at the maximum temperature at 2 °C/h with ~4.44 %Re is the ΣC_{1-5}max. For each g of organic carbon of the initial coal, the amount of organic carbon in the generated gaseous hydrocarbons is $0.8 \times \Sigma C_{1-5}$ assuming that the averaged carbon content in these gas components is 80%. The amount of organic carbon in generated CO_2 is "$S_{CO2} \times 12/44$" in mg TOC/g TOC (formula 1).

GGP values for the residual solid of the seven coals at 1.87–4.44 %Re at 2 °C/h and 1.95–3.84 %Re at 20 °C/h are shown in Fig. 8b and d, respectively. GGP values vary within a narrow range for the seven coals at the same maturities. This result demonstrates that, at the highly post-mature stage with >1.87 %Re, coals with similar maturities have similar gas generation potentials even though these coals have very different initial HI values at immature or marginally mature stages. David Curry (2019, personal communication) suggested that there are significant changes in the composition, structure, and reaction mechanisms in coals and kerogens as maturation progresses, and as the organic matter evolves from main-stage thermal cleavage reactions of the primary organic matter and gradually becomes more condensed and dominated by reactions of the secondary, neo-formed refractory organic matter from condensation reactions involving both the kerogen matrix and the non-expelled organic matter. This result shows that at high

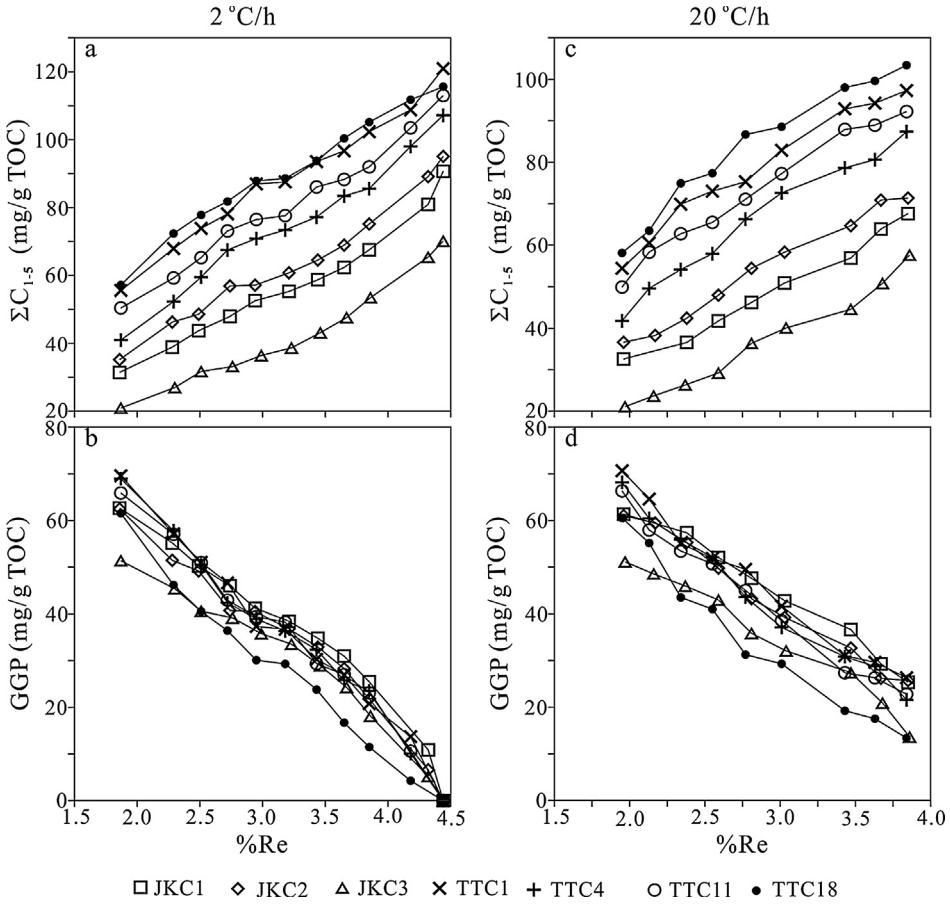

Fig. 8. Gas yields (ΣC_{1-5}) of the seven coals and gas generative potentials (GGP) for the residual solid of the seven coals at maturities of 1.87–4.44 %Re at a heating rate of 2 °C/h (a and b) and for 1.95–3.84 %Re at a heating rate of 20 °C/h (c and d).

levels of maturity (~2 %Re), organic matter acquires an increasingly uniform composition regardless of source.

GGP values are substantially higher than QIh or HIh for the residual solid of the seven coals recovered from confined pyrolysis experiments at 443–479 °C at 2 °C/h (1.87–2.51 %Re). Furthermore, it is noteworthy that products released from residual solids at a highly post-mature stage in Rock-Eval pyrolysis are overwhelmingly aromatic components, as demonstrated by pyrolysis-gas chromatograms of post-mature coals (e.g., Boreham et al., 1999) and residual solids of coals in confined pyrolysis experiments (e.g., Mansuy et al., 1995; Mansuy and Landais, 1995). The differences between GGP and QIh values for the residual solids of the seven coals are shown in Table 2. For residual solids at 443, 467 and 479 °C at 2 °C/h, the differences are 28.0, 21.1 and 20.5 mg/g TOC respectively for coal TTC18, while they are within the range 33.7–42.8, 32.6–39.3 and 31.3–36.3 mg/g TOC respectively for the other six coals. This discrepancy between GGP and QIh may be partly ascribed to the difference in thermal stress level between Rock-Eval pyrolysis and confined pyrolysis. The %Re value for Rock-Eval pyrolysis at 600 °C at 25 °C/min is 2.25 while it is 4.44 for the same temperature in the confined pyrolysis heated at 2 °C/h. As documented in previous studies (e.g., McNeil and BeMent, 1996; Erdmann and Horsfield, 2006; Alexander et al., 2011; Pan et al., 2012; Li et al., 2013, 2016), methane formation in the confined pyrolysis of coals results from the interaction between kerogen and free oil components, rather than from the independent cracking of kerogen and free oil. The difference between GGP and QIh values may also be partly ascribed to the different formation mechanisms of methane between confined and open pyrolysis. This result indicates that at a highly post-mature stage, coals still have the capability to generate a significant amount of methane with maturity further increasing even if they have very low S1 + S2 values (QI < 15 mg HC/g TOC).

Behar et al. (1997) also observed a systematic underestimation of the late production of methane in Rock-Eval pyrolysis in comparison to that obtained in a closed system and suggested that this underestimation is partly due to a too low final temperature and to competitive formation of methane and molecular hydrogen in Rock-Eval pyrolysis. The results of the present study are consistent with the conclusions made by Behar et al. (1997).

Table 2
Differences between GGP and QIh for residual solids heated at 443–479 °C at 2 °C/h with %Re values of 1.87–2.51.

	443 °C	467 °C	479 °C
JKC1	40.5	37.8	34.4
JKC2	36.2	35.2	33.6
JKC3	33.7	32.6	32.0
TTC1	42.8	38.7	36.2
TTC4	39.3	39.3	31.3
TTC11	39.8	37.2	36.3
TTC18	27.9	21.0	20.5

All data in "mg HC/g TOC".

4.3. Kinetic modelling for petroleum generation

4.3.1. Kinetic parameters for oil generation (S_O)

Petroleum generation from kerogen is generally described using a set of parallel first-order reactions with a single frequency factor and a distribution of activation energies (e.g., Ungerer and Pelet,

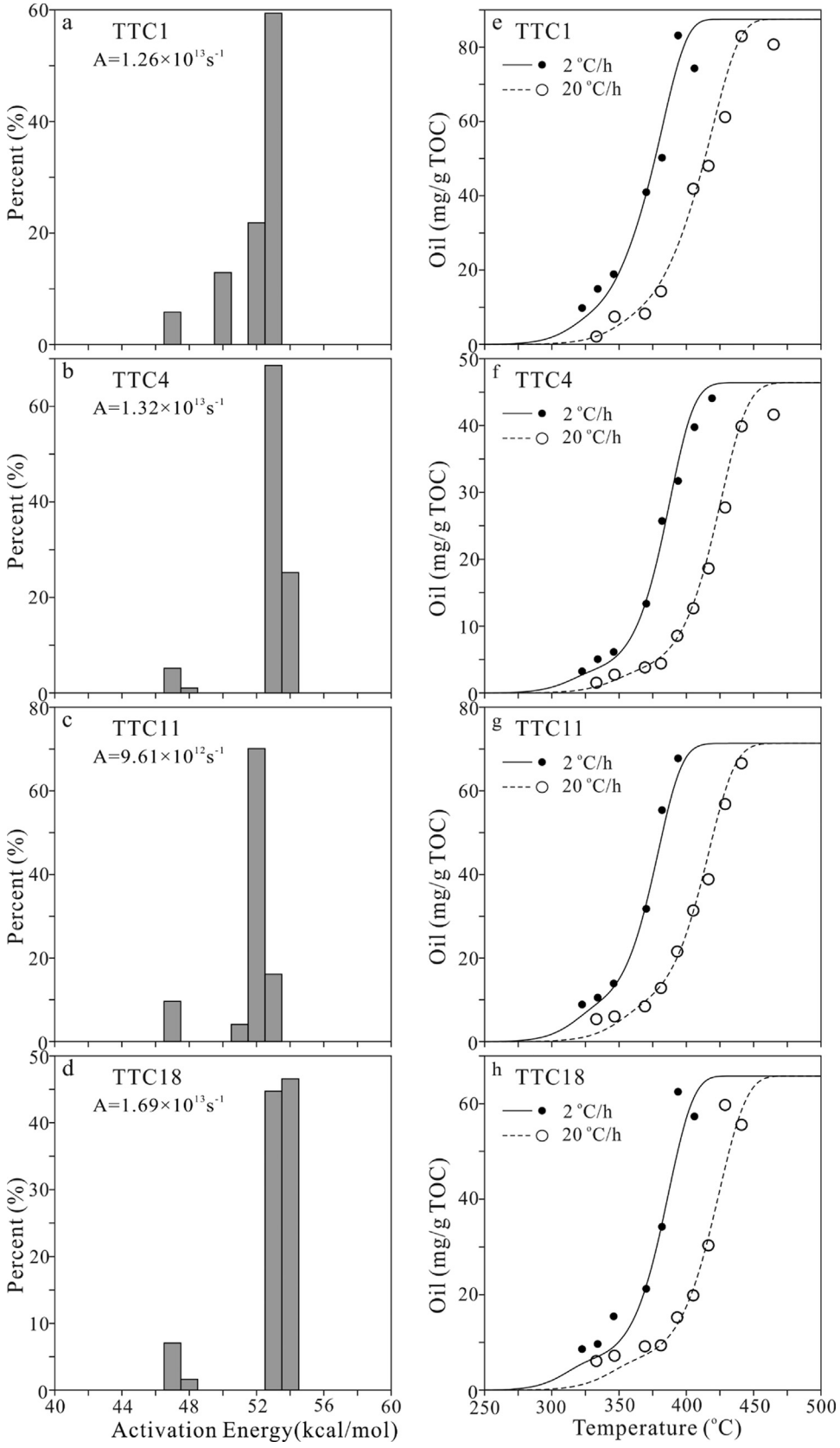

Fig. 9. Activation energy distributions and frequency factors for oil generation (left), and the fits of calculated cumulative amounts of oil with measured results (right) for the four Triassic coals TTC1, TTC4, TTC11 and TTC18.

1987; Espitalié et al., 1988; Schenk and Horsfield, 1993; Tang et al., 1996; Behar et al., 1997; Peters et al., 2006, 2015). In the present study, kinetic parameters were determined for the generation of oil and hydrocarbon gases using Kinetics 2000 software (Version 1.11), developed by Burnham and Braun (1999). Among the seven coal samples, coals JKC1, JKC2 and JKC3 are ineffective oil source rocks, and therefore we only determined the kinetic parameters for oil generation from remaining four coals.

For coals TTC1, TTC4, TTC11 and TTC18, the measured maximum S_O values are 83.2, 44.1, 67.8 and 62.5 mg/g at 2 °C/h and 83.0, 41.6, 66.6 and 59.7 mg/g TOC at 20 °C/h, respectively. The maximum S_O values for modelling oil generation from these four coals are 87.5 (83.2/0.95), 46.4 (44.1/0.95), 71.3 (67.8/0.95) and 65.8 (62.5/0.95) mg/g TOC respectively, assuming that the measured maximum S_O values represents 95% of the transformation ratio considering the overlap between oil generation and cracking (e.g., Dieckmann et al., 2000; Erdmann and Horsfield, 2006). Kinetic parameters for oil generation from these four coals were optimized using the Kinetics 2000 software and are shown in Fig. 9a–d. The fits of the cumulative oil yields calculated from the kinetic parameters and measured from confined pyrolysis experiments are shown in Fig. 9e–h. The weighted averaged activation energies are 52.04, 52.89, 51.64 and 52.96 kcal/mol with the frequency factors $1.26 \times 10^{13}\ s^{-1}$, $1.32 \times 10^{13}\ s^{-1}$, $9.61 \times 10^{12}\ s^{-1}$ and $1.69 \times 10^{13}\ s^{-1}$ respectively for coals TTC1, TTC4, TTC11 and TTC18 (Table 3). The differences in kinetic parameters for oil generation among the four coals are minor and well within the analytical uncertainty. We determined a generalized kinetic model for oil generation for the Upper Triassic Taliqike Formation coals (TTC) using the averaged oil yields of these four samples (Fig. 10). The maximum oil yield for the generalized model is 67.8 mg/g TOC the activation energy is 52.4 kcal/mol with the frequency factor $1.26 \times 10^{13}\ s^{-1}$ TC (Table 3).

Narrow distributions of activation energy for oil generation were modeled for the individual coals TTC1, TTC4, TTC11 and TTC18 and their average (TTC), indicating that the precursors for oil generation have similar chemical bonds. Killops et al. (1998) suggested that oil from coals are characteristically paraffinic and can be considered to derive from a polymethylene component. In addition to the precursors, this distribution pattern can be also ascribed to the following two causes:

(1) Previous studies have suggested or demonstrated that kerogen or pyrobitumen catalyzes the cracking of oil and wet gases (Greensfelder et al., 1949; Smith et al., 1989; Pepper and Dodd, 1995; Schenk et al., 1997; Dieckmann et al., 1998; Hill et al., 2007; Alexander et al., 2009, 2011; Pan et al., 2012; Jin et al., 2013; Li et al., 2013, 2016).
(2) In kerogen pyrolysis experiments and natural systems, oil components are both released from kerogen and incorporated into kerogen (e.g., McNeil and BeMent, 1996; Boreham et al., 1999; Dieckmann et al., 2006; Erdmann and Horsfield, 2006; Pan et al., 2012; Li et al., 2013, 2016).

Given the influence of the solid organic matrix on oil cracking and the fact that coals generally have a lower ratio of oil/solid kero-

Table 3
Kinetic parameters for oil and gas formations from Triassic-Jurassic coals.

Ea	Fraction (%)	Ea	Fraction (%)	Ea	Fraction (%)	Ea	Fraction (%)	Ea	Fraction (%)
TTC1		TTC4		TTC11		TTC18		TTC	
Oil generation									
$A = 1.26 \times 10^{13}\ s^{-1}$		$A = 1.32 \times 10^{13}\ s^{-1}$		$A = 9.61 \times 10^{12}\ s^{-1}$		$A = 1.69 \times 10^{13}\ s^{-1}$		$A = 1.26 \times 10^{13}\ s^{-1}$	
47	5.83	47	5.17	47	9.63	47	7.07	47	5.27
50	12.9	48	1.03	51	4.12	48	1.64	48	3.02
52	21.9	53	68.6	52	70.1	53	44.7	49	3.74
53	59.4	54	25.2	53	16.1	54	46.6	53	88.0
Gas generation (ΣC_{1-5})									
$A = 8.22 \times 10^{13}\ s^{-1}$		$A = 1.66 \times 10^{14}\ s^{-1}$		$A = 1.67 \times 10^{14}\ s^{-1}$		$A = 9.16 \times 10^{13}\ s^{-1}$		$A = 9.97 \times 10^{13}\ s^{-1}$	
51	0.22	56	3.69	55	5.06	57	11.4	55	3.82
55	8.69	58	11.0	58	15.8	58	7.88	57	10.4
56	2.33	59	7.17	60	6.20	59	19.0	59	19.6
59	26.0	61	15.5	61	16.9	61	10.9	61	9.41
61	9.40	62	2.22	64	13.7	62	6.31	62	7.93
62	8.35	64	7.83	67	14.8	63	10.2	63	1.41
65	17.6	65	16.0	72	6.50	64	5.66	64	9.89
71	27.4	67	5.19	73	21.0	67	9.70	66	11.1
		72	30.1			68	2.06	71	18.4
		73	1.34			71	16.7	72	8.18
						72	0.22		
JKC1		JKC2		JKC3		JKC			
Gas generation (ΣC_{1-5})									
$A = 1.17 \times 10^{14}\ s^{-1}$		$A = 1.22 \times 10^{14}\ s^{-1}$		$A = 8.25 \times 10^{13}\ s^{-1}$		$A = 1.20 \times 10^{14}\ s^{-1}$			
51	0.48	51	0.03	51	0.8	51	0.55		
53	2.13	54	4.75	54	2.17	54	1.83		
55	3.9	55	1.85	55	4.56	55	5.13		
57	0.71	58	15.8	58	12.2	58	6.00		
58	12.2	60	9.98	59	3.83	59	14.8		
59	8.12	61	4.52	61	3.11	62	7.75		
62	7.99	64	17.2	62	5.48	64	7.68		
64	9.90	65	6.14	64	17.5	65	13.5		
65	10.4	71	39.8	69	27.9	71	42.8		
71	44.3			72	22.5				

Ea: activation energies in kcal/mol; A: frequency factor.

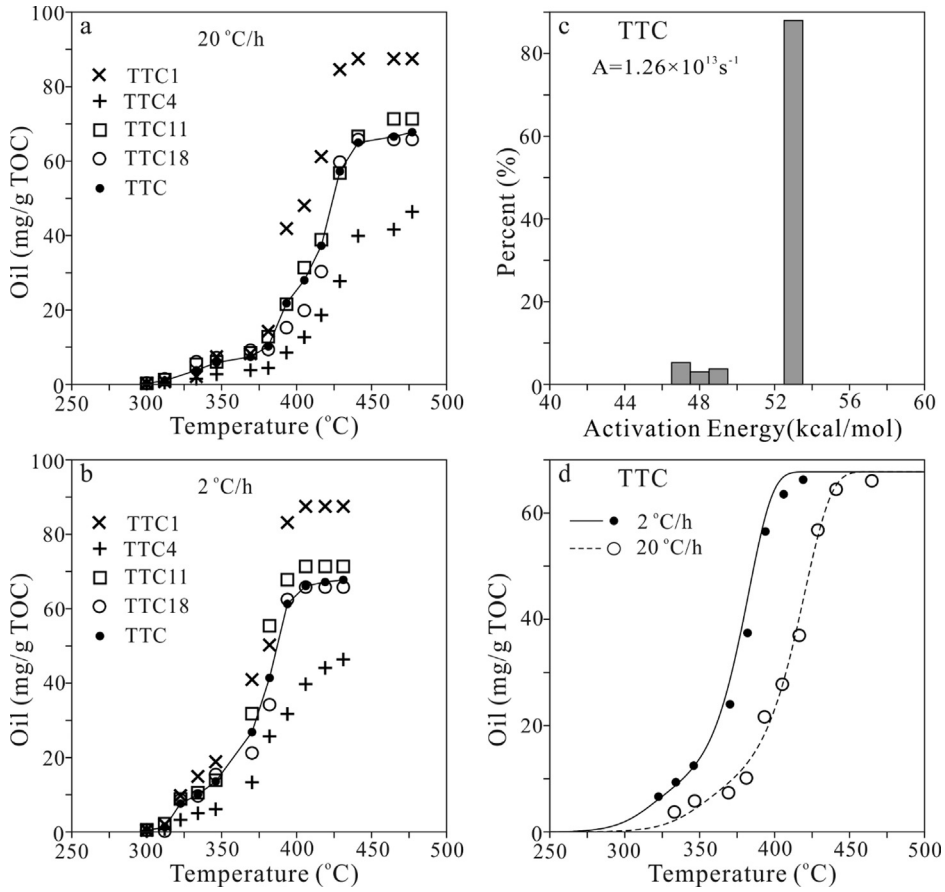

Fig. 10. Oil yields and the averaged values of the four Triassic coals at 20 °C/h (a) and 2 °C/h (b); activation energy distribution and frequency factor for oil generation for the generalized coal TTC (c), determined using the averaged oil yields of the four Triassic coals (d).

gen than oil-prone source rocks, the maturities and temperatures for the maximum accumulative oil yields (S_O) will be lower compared to oil-prone source rocks. Erdmann and Horsfield (2006) demonstrated that the temperatures for the maximum oil yield (ΣC_{6+}) is significantly lower for gas-prone kerogen Heather (HI 146 mg HC/g TOC) than oil-prone kerogen Draupne (HI of 555 mg HC/g TOC). In the present experiments, %Re values for the maximum accumulative oil yields (S_O) mainly range from 1.17 to 1.30, consistent with the pyrolysis experiments on coals conducted by Li et al. (2013), which are lower than pyrolysis experiments on oil-prone kerogens conducted by Xiang et al. (2016). At temperatures and maturities higher than those for the maximum accumulative oil yields (S_O), oil generation rate is lower than the rate of oil-cracking and incorporation to kerogen. In this case, oil generation is actually invalid because the amount of the generated oil is unable to be determined and incorporated into the modeling of kinetic parameters for oil generation. It can be expected that in natural systems oil generation and expulsion is actually completed when the oil generation rate is lower than the rate of oil cracking and incorporation into kerogen. As a result, the distributions of activation energies for oil generation from coals generally do not include an E_a distribution with higher values.

4.3.2. Kinetic parameters for generation of total gaseous hydrocarbons (ΣC_{1-5})

Kinetic parameters for the generation of total gaseous hydrocarbons (ΣC_{1-5}) for the seven coals were determined using Kinetics 2000 software (version 1.11; Burnham and Braun, 1999), based on the measured yield data at the two heating rates of 20 °C and 2 °C/h in confined pyrolysis. The obtained kinetic parameters and the fits of the cumulative yields of total gaseous hydrocarbons calculated from the kinetic parameters and measured from confined pyrolysis experiments are shown in Table 3 and Figs. 11 and 12. The weighted averaged activation energies for gas generation are 64.7, 65.2 and 65.3 kcal/mol with frequency factors $1.17 \times 10^{14}\ s^{-1}$, $1.22 \times 10^{14}\ s^{-1}$ and $8.25 \times 10^{13}\ s^{-1}$, respectively for coals JKC1, JKC2 and JKC3 within the Middle Jurassic Kezilenuer Formation (J_2k), and 63.4, 65.0, 64.7 and 62.8 kcal/mol with frequency factors $8.21 \times 10^{13}\ s^{-1}$, $1.66 \times 10^{14}\ s^{-1}$, $1.67 \times 10^{14}\ s^{-1}$ and $9.16 \times 10^{13}\ s^{-1}$, respectively for coals TTC1, TTC4, TTC11 and TTC18 within the Upper Triassic Taliqike Formation (T_3t). We further determined the kinetic parameters for two generalized samples, JKC and TTC, using the averaged gas yields for the three coals within the Middle Jurassic Kezilenuer Formation (J_2k) and four coals within the Upper Triassic Taliqike Formation (T_3t), to predict gas generation from coal beds within these two formations (Figs. 13 and 14). Kinetic parameters for gas generation and the fits of the cumulative yields of total gaseous hydrocarbons calculated from the kinetic parameters and measured from confined pyrolysis experiments for these two generalized coals JKC and TTC are shown in Table 3 and Figs. 13 and 14.

4.3.3. Generation of gaseous hydrocarbons in a natural (semi-open) system

For coal pyrolysis experiments in a confined (closed) system, both kerogen and the generated oil components produce gaseous hydrocarbons via complicated reaction pathways. In natural (semi-open) systems, oil expulsion occurs from the coals when the amount of the generated oil is higher than the threshold value for oil expulsion, (e.g., 40 mg/g TOC; Killops et al., 1998). Oil expul-

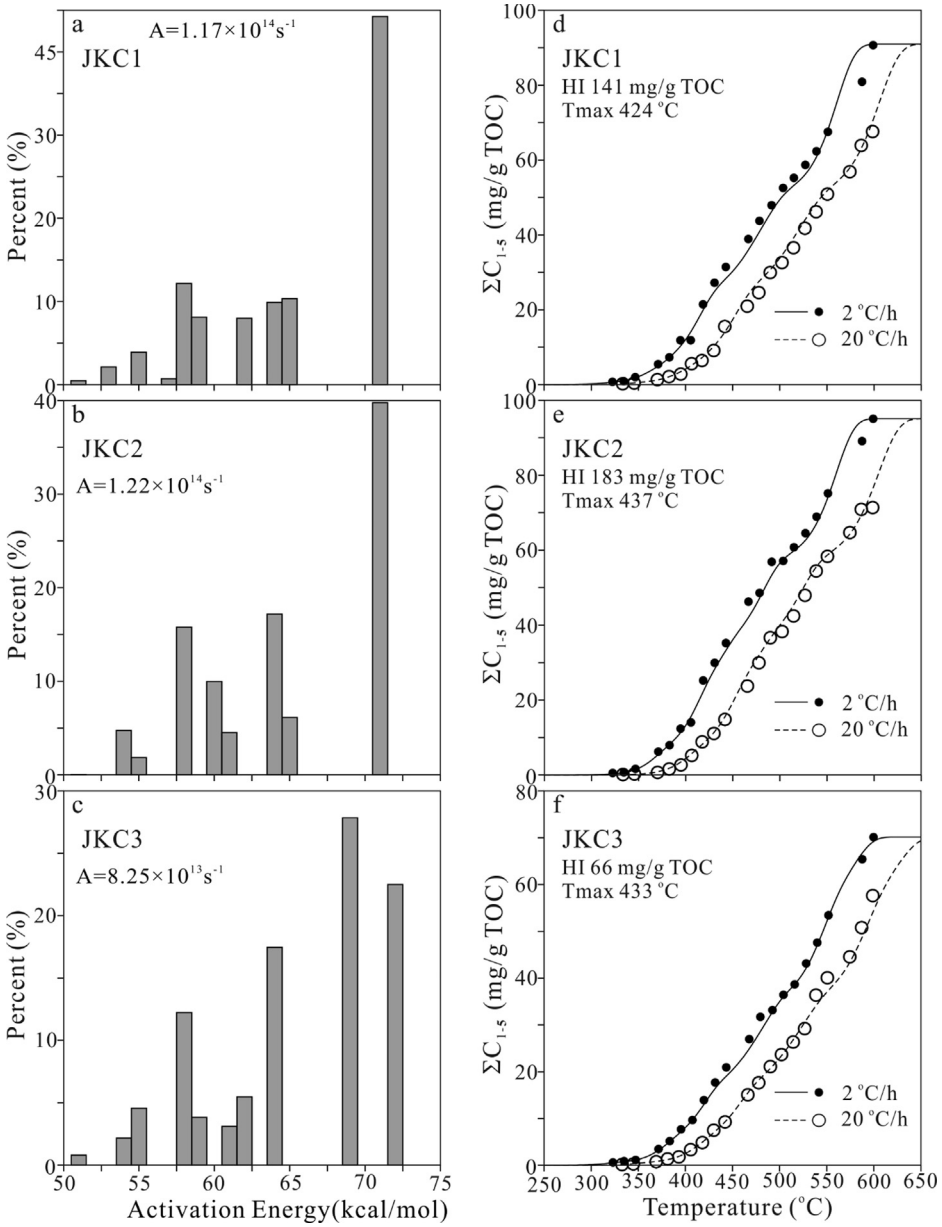

Fig. 11. Activation energy distributions and frequency factors for gas generation (left), and the fits of calculated cumulative amounts of gases with measured results (right) for the three Jurassic coals.

sion leads to the reduction of the maximum accumulative yield of gaseous hydrocarbons generated from the coal source rocks.

For coals JKC1, JKC2 and JKC3 within the middle Jurassic Kezilenuer Formation (J_2k), the maximum accumulative oil yields are lower than the threshold value for oil expulsion. Oil expulsion does not occur in the natural system. The maximum accumulative gas yields in the natural system are the same as in confined experiments. In contrast, for coals TTC1, TTC4, TTC11 and TTC18 within the Upper Triassic Taliqike Formation (T_3t), the maximum accumulative oil yields are higher than the threshold value for oil expulsion. Oil expulsion would occur in the natural system during the oil generation stage. Xiang et al. (2016) presented an approach to predict the amount of expelled oil and the accumulative yield of gaseous hydrocarbons after oil expulsion. The maximum accumulative gas yields in the natural system for the four Triassic coals can be calculated using this method.

4.4. Hydrocarbon generation from Kuqa depression

Petroleum generation from coals within the Upper Triassic Taliqike Formation (T_3t) and the middle Jurassic Kezilenuer Formation (J_2k) was modelled using kinetic parameters of the generalized coals TTC and JKC (Table 3) under a geological condition of 5 °C/My (Table 4, Fig. 15). The amounts of oil and gaseous hydrocarbons are very low at %Re values of 0.65 and 1.00, the generalized thresholds for onset and peak oil generative window for both coals. Coal TTC has an oil yield >40 mg/g TOC at 1.08 %Re and 158.6 °C, reaching the threshold for oil expulsion (Killops et al., 1998). In a closed system without oil expulsion, coal TTC would have gas yield higher than 20 mg/g TOC at 1.52 %Re and 183.8 °C, reaching the threshold for gas expulsion (Pepper and Corvi, 1995b). However, in a semi-open system with efficient oil expulsion, coal TTC would reach the threshold for gas expulsion at 1.59 %Re and 186.6 °C. Coal

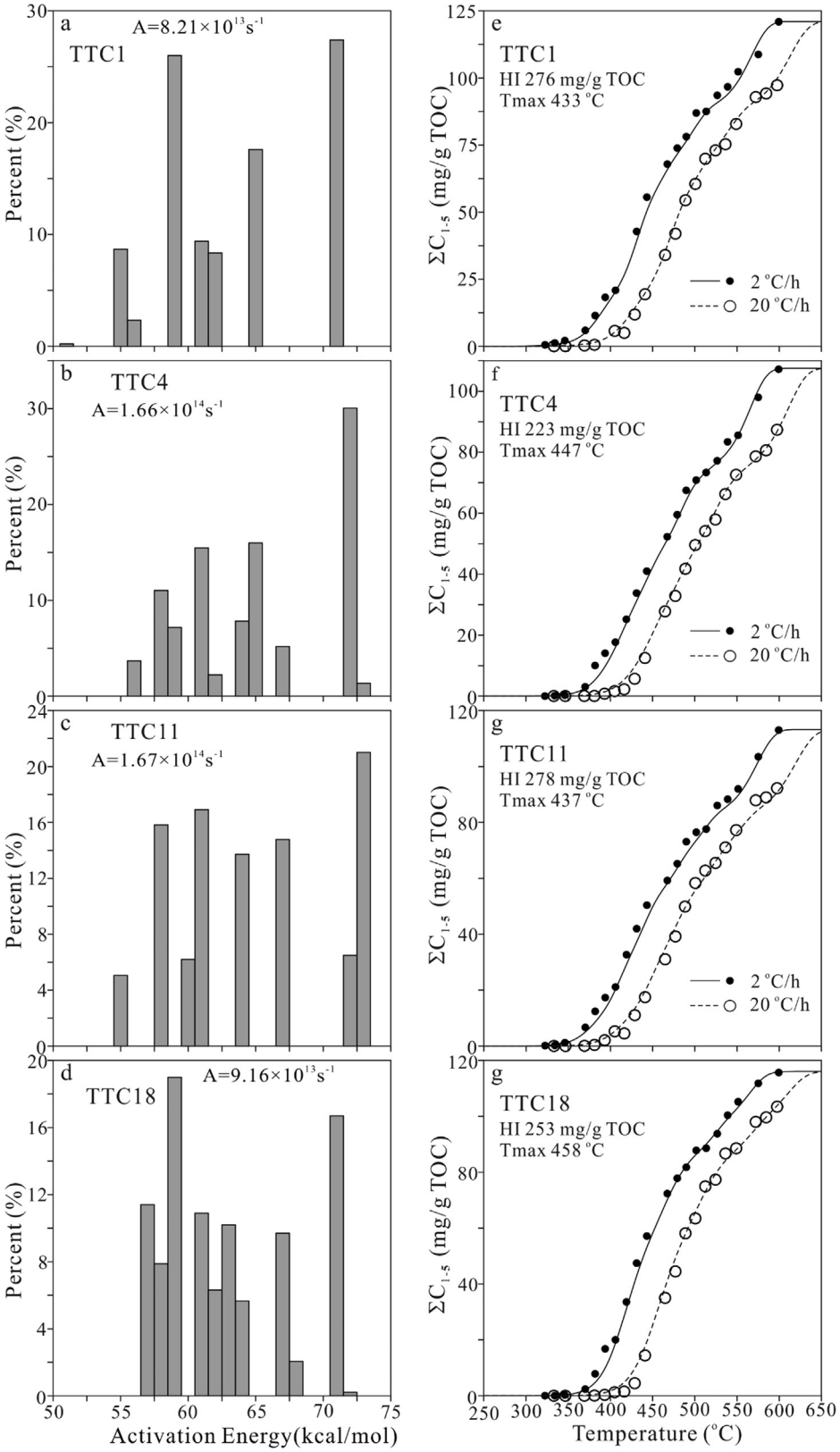

Fig. 12. Activation energy distributions and frequency factors for gas generation (left), and the fits of calculated cumulative amounts of gases with measured results (right) for the four Triassic coals.

JKC reaches the threshold for gas expulsion at 1.76 %Re and 193.6 °C (Table 4, Fig. 15).

The burial and thermal histories for the Triassic–Jurassic strata in the central area of the Kuqa Depression can be divided into two stages: a slow burial from the sedimentation to Neogene (12 Ma) and a rapid burial after about 12 Ma (Liang et al., 2003; Zhao et al., 2005). During the first stage, these strata were buried over 6 km deep with temperature over 160 °C and up to 1.50 %Ro. At

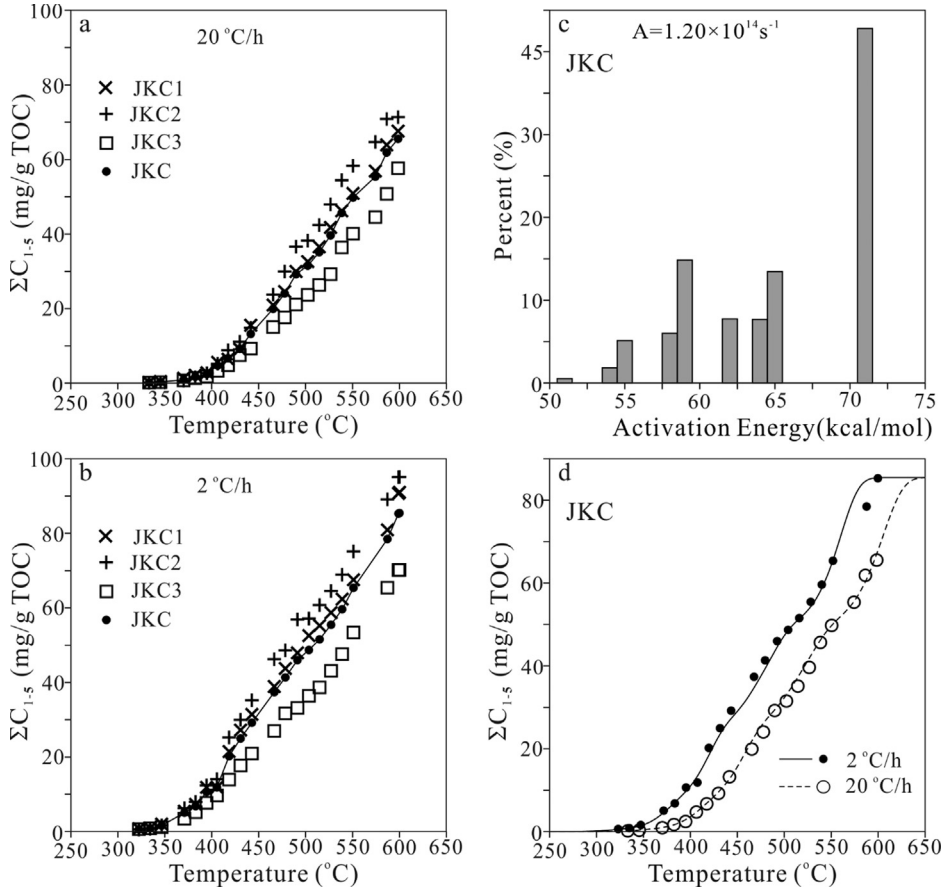

Fig. 13. Gas yields and the averaged values of the three Jurassic coals at 20 °C/h (a) and 2 °C/h (b), activation energy distribution and frequency factor for gas generation for the generalized coal JKC (c), determined using the averaged gas yields of the three Jurassic coals (d).

the second stage, these strata were buried over 10 km deep with temperature over 280 °C and over 2.50 %Ro (Liang et al., 2003; Zhao et al., 2005). Furthermore, a rapid uplift and erosion likely occurred in the whole Kuqa Depression during the Quaternary based on tectonic and geographic settings (Fig. 1; Zhang et al., 2011; Guo et al., 2016), so it is difficult to reconstruct the burial histories and estimate the maturities for the Triassic–Jurassic coaly source rocks, which are possibly even higher than those suggested by Zhao et al. (2005).

The maturities of the Triassic–Jurassic source rocks can be also inferred from the dryness ratios ($C_1/\Sigma C_{1-5}$) of gaseous hydrocarbons from gas reservoirs in the depression. This ratio ranges from 0.96 to 1.00 for major giant gas fields in the Kelasu Structural Belt (KSB) in the central area of Kuqa depression (Zhao et al., 2005; Zhang et al., 2011; Wang, 2014; Guo et al., 2016). In particular, this ratio ranges from 0.996 to 1.000 for gas fields KL2 and KS2, the two largest gas fields in this belt, as well as in the whole Tarim Basin (Wang, 2014), suggesting that the source maturities are extremely high. Within this belt, a number of giant gas fields have been found with total in-place gas reserves over 1×10^{12} m^3 (Wang et al., 2013; Wang, 2014). Furthermore, it is expected that additional gas reservoirs with total in-place gas reserves up to 1×10^{12} m^3 could be discovered within this belt in the near future (Wang et al., 2013; Wang, 2014). The elevated maturities (%Ro > 2.0) are crucial for coaly source rocks to generate and expel sufficient gaseous hydrocarbons for the formation of giant gas fields in the Kuqa depression (Table 4 and Fig. 15). Coal TTC within the Upper Triassic Taliqike Formation (T_3t) obviously generated a higher amount of gaseous hydrocarbons than coal JKC within the Middle Jurassic Kezilenuer Formation (J_2k) due to higher gas generative potential and maturity (Fig. 15).

Dieckmann et al. (2006) and Erdmann and Horsfield (2006) documented the enhanced late gas generation from the cracking of highly stable substituents from the recombined bitumen in source rocks with Type III kerogen, and suggested that this type of high maturity methane can be found in the North Sea where source rocks within the Heather Formation are deeply buried at temperature >200 °C and in the Mackenzie Delta where source rocks within the Taglu Sequence or similar sequences have maturities >2.5 %Ro. We conclude that the gas fields KL2 and KS2 in the Kuqa Depression (Fig. 1) are the type of reservoirs that accumulated high maturity methane.

4.5. Mechanism for gas generation at a highly post-mature stage

At 2.19 %Re, gas yields (ΣC_{1-5}) of the generalized coals JKC and TTC models are about 27.5 and 50.5 mg/g TOC, contributing about 32% and 44% of the maximum gas yields of these two coals at 4.44 %Re, respectively (Table 4), consistent with previous studies on coal pyrolysis (Li et al., 2013; Xu et al., 2017). Dieckmann et al. (2006) and Erdmann and Horsfield (2006) suggested that the recombination reactions of liquid products released from Type III kerogen at low levels of maturation result in the formation of a thermally stable bitumen, which is the major source of methane at very high maturity. Li et al. (2013) suggested that in coal pyrolysis experiments the major portion of methane shares a common initial precursor with wet gases, i.e., free and bound liquid alkanes because $\delta^{13}C$ values of the accumulated methane at the maximum

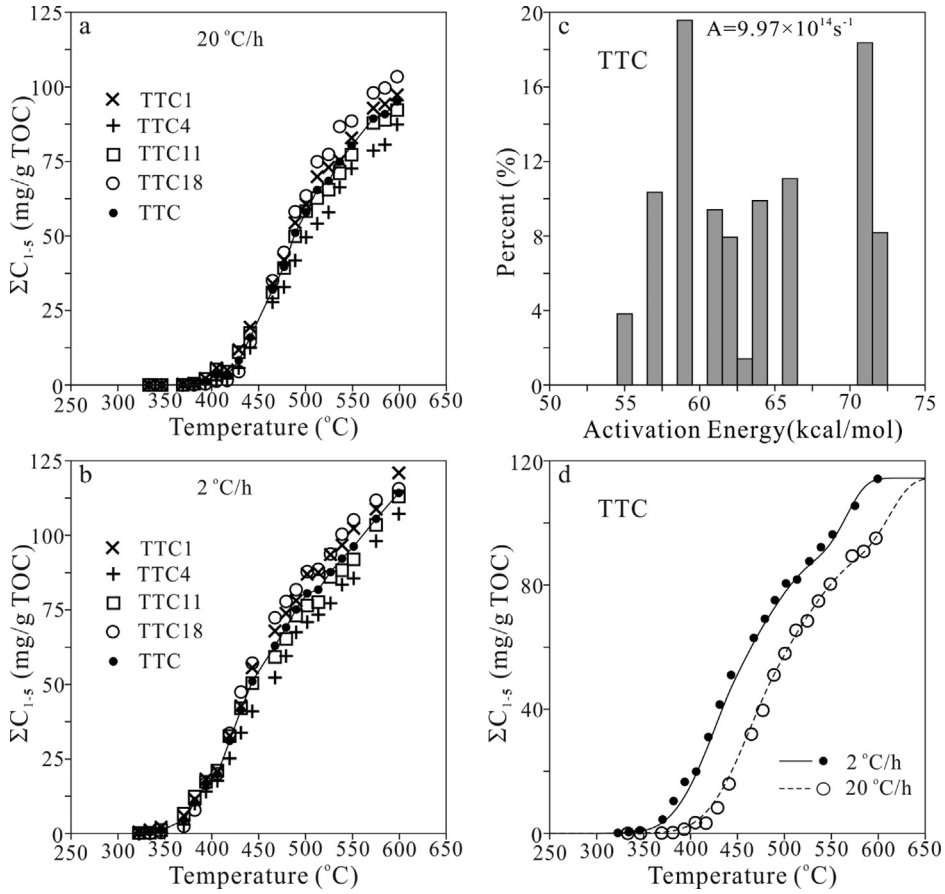

Fig. 14. Gas yields and the averaged values of the four Triassic coals at 20 °C/h (a) and 2 °C/h (b); activation energy distribution and frequency factor for gas generation for the generalized coal TTC (c), determined using the averaged gas yields of the four Triassic coals (d).

Table 4
Accumulative oil and gas yields from JKC and TTC coals at 5 °C/My.

%Re	T (°C)	JKC ΣC_{1-5}-C	TTC S_O-G	TTC S_O-E	TTC ΣC_{1-5}-C	TTC ΣC_{1-5}-SO
0.65	116.6	0.23	4.48	0	0.003	0.002
1.00	154.4	3.01	28.7	0	1.55	1.38
1.08	158.6	4.28	40.7	0.76	2.70	2.41
1.21	167.0	6.73	63.6	24.4	6.48	5.78
1.37	175.0	8.74	67.7	28.7	12.1	10.8
1.52	183.8	13.0	67.8	28.7	20.6	18.4
1.59	186.6	15.1	67.8	28.7	23.7	21.1
1.76	193.6	20.9	67.8	28.7	32.4	28.9
1.99	203.4	25.5	67.8	28.7	44.0	39.2
2.19	210.4	27.5	67.8	28.7	50.3	44.9
2.49	221.6	33.0	67.8	28.7	60.8	54.2
3.00	238.4	44.3	67.8	28.7	73.5	65.6
3.50	255.2	49.8	67.8	28.7	83.6	74.6
4.01	276.2	59.7	67.8	28.7	90.4	80.6
4.44	300	85.3	67.8	28.7	112.9	100.7

ΣC_{1-5}-C: gas yield (ΣC_{1-5}) in closed system; ΣC_{1-5}-SO: gas yield (ΣC_{1-5}) in semi-open system; S_O-G: the amount of generated oil; S_O-E: the amount of expelled oil; All yield data in mg/g TOC.

4.44 %Re are close to those of the initial wet gases, especially propane). According to the reaction model of McNeil and BeMent (1996), alkane moieties attached to aromatic rings in the solid kerogen cleave preferentially under thermal stress at the position between the first and second carbon atoms leading to a methyl group attaching to the aromatic rings and formation of an alkyl radical with one carbon shorter than the original alkyl group. Further rupture of the methyl group from the aromatic rings leads to the formation of methane. As a result, methane is the dominant component in gaseous hydrocarbons generated from source rocks.

The maximum accumulative oil yields are substantially lower than the maximum accumulative gas yields in the present study (Table 4, Fig. 15), as well as in previous studies on coal pyrolysis experiments (Li et al., 2013; Xu et al., 2017), suggesting that liquid alkanes generated in the oil generative window only contribute a minor portion of the bound alkyl groups in the initial coals. The major portion of the initial bound alkyl moieties remains attaching to aromatic rings in residual kerogen even at high maturity up to 2.20 %Re with further increases in the precursor for methane formation as maturity increases. As a consequence, oil generation

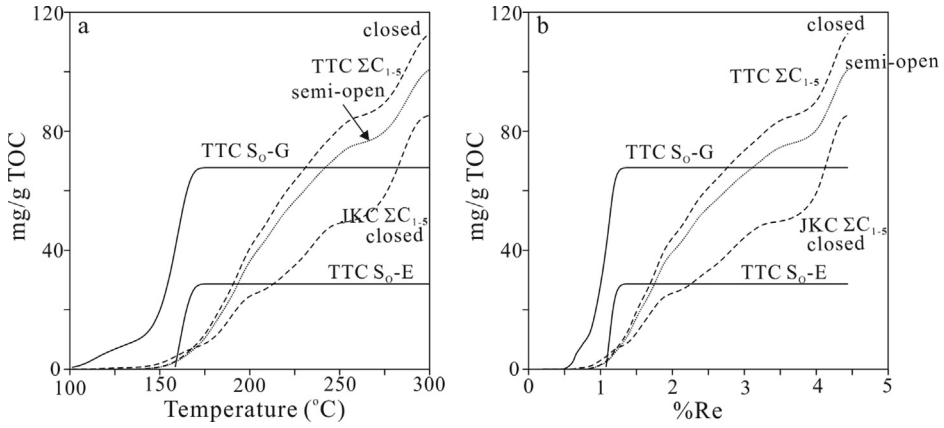

Fig. 15. The predicted cumulative amounts of oil generated and expelled, and total gaseous hydrocarbons (ΣC_{1-5}) generated in closed and semi open systems for both the generalized coals JKC and TTC under geological conditions of 5 °C/my vs temperature (left) and %Re (right). S_O-G: the cumulative amount of oil generated; S_O-E: the cumulative amount of oil expelled.

and expulsion occurs within a narrow maturity range (Fig. 15), due to the narrow distribution of activation energies for humic coals (Fig. 9). It can be envisaged that within the early oil generative window, the released alkyl radical can capture a hydrogen radical and form an alkane. At high maturity within the gas generative window, this released alkyl radical may immediately attach back to aromatic rings of solid kerogen. In addition, the free alkanes can attach back to solid kerogen (McNeil and BeMent, 1996; Boreham et al., 1999; Erdmann and Horsfield, 2006; Li et al., 2013, 2016).

5. Conclusions

In confined pyrolysis experiments, four coals (TTC1, TTC4, TTC11 and TTC18) within the Triassic Taliqike Formation (T_3t) with HI ranging from 223 to 278 mg HC/g TOC have maximum oil yields ranging from 46.4 to 87.5 mg/g TOC and maximum gas yields (ΣC_{1-5}) ranging from 107.2 to 120.9 mg/g TOC. Three coals (JKC1, JKC2 and JKC3) within the Jurassic Kezilenuer Formation (J_2k) with HI ranging from 57 to 183 mg HC/g TOC have maximum oil yields ranging from 14.3 to 39.8 mg/g TOC and the maximum gas yields (ΣC_{1-5}) ranging from 70.1 to 95.1 mg/g TOC.

Mass balance results from within the oil generative window demonstrate that only a portion (38–53%) of the releasable moieties measured by Rock-Eval pyrolysis contributed to the formation of oil and gaseous hydrocarbons, while the other portion (47–62%) of these moieties was rearranged and incorporated into polyaromatic residual solids.

At high maturities (%Re > 1.87), gas generative potentials (ΣC_{1-5}, GGP) for the residual solid are very similar among the seven coals, and are substantially higher than the QI values ((S1 + S2)/TOC) of the residual solid with the differences ranging from 20 to 40 mg/g TOC. This can be ascribed to the differences both in methane formation mechanisms and thermal stress level between Rock-Eval pyrolysis (2.25 %Re) and confined pyrolysis (4.44 %Re).

For the four Triassic coals that are effective oil source rocks with maximum oil yield >40 mg/g TOC, the weighted average activation energies for oil generation range from 51.6 to 53.0 kcal/mol with frequency factors ranging from 9.61×10^{12} s^{-1} to 1.69×10^{13} s^{-1}. The distributions of activation energies for oil generation from these four coals are narrow, indicating that the precursors possess similar chemical bonds that are cleaved for oil generation. This feature can be also partly ascribed to the concept that only a limited portion of the bound alkanes in the initial coal can be released as oil components.

The weighted average activation energies for gas generation range from 64.7 to 65.3 kcal/mol with frequency factors ranging from 8.25×10^{13} s^{-1} to 1.22×10^{14} s^{-1} for the three Jurassic coals and range from 62.8 to 65.0 kcal/mol with frequency factors ranging from 8.21×10^{13} s^{-1} to 1.67×10^{14} s^{-1} for four Triassic coals. Only a minor portion of gaseous hydrocarbons, about 32% and 44%, respectively for the Jurassic coals and Tisassic coals is generated at up to 2.19 %Re while the major portion is generated at higher maturities.

Kinetic parameters of the generalized coals JKC and TTC for oil and gas generation were determined from the average yields of the three Jurassic coals and four Triassic coals, respectively. Under natural conditions with aheating rate of 5 °C/My, the generalized Jurassic coal JKC and Triassic coal TTC can be effective gas source rocks with gas yield >20 mg/g TOC at %Re >1.76 and 1.59, respectively. The abundant gaseous hydrocarbons found in the Kuqa Depression can be mainly ascribed to high maturities of coal source rocks (%Ro > 2.0), especially Triassic coal source rocks, in combination with excellent seal of thick salt and gypsum for the gas reservoirs.

Acknowledgements

This study was jointly funded by the National S&T Major Project of China (Grant No. 2017ZX05008-002-030), the National Natural Science Foundation of China (Grant 41572107) and the Strategic Priority Research Program of the Chinese Academy of Sciences (XDA14010104). We are very grateful to Drs. Alan Burnham and David Curry for their helpful comments, and editors John Volkman and Cliff Walters for their editorial work and language improvements for our paper. This is contribution No. IS-2689 from GIGCAS.

Appendix A. Analyzed and calculated parameters

	Description
	Gross Parameters
TOC	Total organic carbon content (%) analyzed by Leco-230C/S
%Ro	Vitrinite reflectance
	Rock-Eval Pyrolysis using IFP Rock–Eval 6
S1	Free or adsorbed hydrocarbons (mg HC/g Rock)
S2	Hydrocarbons generated by pyrolytic degradation of the kerogen (mg HC/g Rock)

Appendix A (*continued*)

	Description
S3	CO_2 generated by pyrolytic degradation of the kerogen (mg CO_2/g Rock)
Tmax	Temperature corresponding to the maximum of hydrocarbon generation (°C)
HI	Hydrogen Index = S2/TOC (mg HC/g TOC)
QI	Quality Index = (S1 + S2)/TOC (mg HC/g TOC)
OI	Oxygen Index = S3/TOC (mg CO_2/g TOC)
	Confined Pyrolysis Yields (mg/g TOC)
ΣC_{1-5}	Yield of total hydrocarbon gases
ΣC_{8+}	Yield of liquid components measured from gas chromatograms using internal standards
S_O	Oil yield calculated from ΣC_{8+} using a correction factor 1.776 (1/0.563)
S_{OG}	Total yield of oil and hydrocarbon gases = $\Sigma C_{1-5} + S_O$
S_{CO2}	Yield of CO_2
	Calculated Parameters
QIR	Quality index reduction values calculated from formula (1)
QOGR	Ratio of QIR to S_{OG} (QIR/S_{OG})
GGP	Gas generative potential (mg/g TOC) calculated from formula (2)

Appendix B. Supplementary materials

Supplementary data to this article can be found online at https://doi.org/10.1016/j.orggeochem.2019.04.007.

Associate Editor–**Clifford Walters**

References

Alexander, R., Dawson, D., Pierce, K., Murray, A., 2009. Carbon catalyzed hydrogen exchange in petroleum source rocks. Organic Geochemistry 40, 951–955.

Alexander, R., Berwick, L.J., Pierce, K., 2011. Single carbon surface reactions of 1-octadecene and 2,3,6-trimethylphenol on activated carbon: implications for methane formation in sediments. Organic Geochemistry 42, 540–547.

An, Q., Zhang, Z., Wu, B., Wang, X., 2016. Coal reservoir characteristics and mining technology of Kuqa-Bay coalfield. Xinjiang. Xinjiang Geology 34 (2), 286–290 (in Chinese).

Behar, F., Vandenbroucke, M., Tang, Y., Marquis, F., Espitalié, J., 1997. Thermal cracking of kerogen in open and closed systems: determination of kinetic parameters and stoichiometric coefficients for oil and gas generation. Organic Geochemistry 26, 321–339.

Boudou, J.P., Espitalié, J., Bimer, J., Salbut, P.D., 1994. Oxygen groups and oil suppression during coal pyrolysis. Energy & Fuels 8, 972–977.

Boreham, C.J., Horsfield, B., Schenk, H.J., 1999. Predicting the quantities of oil and gas generated from Australian Permian coals, Bowen Basin using pyrolytic methods. Marine and Petroleum Geology 16, 165–188.

Burnham, A.K., Braun, R.L., 1999. Global kinetic analysis of complex materials. Energy & Fuels 13, 1–21.

Burnham, A.K., Braun, R.L., 2017. Simple relative sorptivity model of petroleum expulsion. Energy & Fuels 31, 9308–9318.

Burnham, A.K., Schmidt, B.J., Braun, R.L., 1995. A test of the parallel reaction model using kinetic measurements on hydrous pyrolysis residues. Organic Geochemistry 23, 931–939.

Curry, D.J., 1995. The pyrolysis yield index: a rapid and reproducible technique for estimating the oil generation potential of coals and terrigenous kerogens. In: Grimalt, J.O., Dorronsoro, C. (Eds.), Organic Geochemistry: Developments and Applications to Energy, Climate, Environment and Human History, Selected papers from the 17th International Meeting on Organic Geochemistry, pp. 763–766.

Curry, D.J., Bohacs, K.M., Diessel, C.F.K., Gammidge, L.C., Rigby, R., 1995. Sequence stratigraphic and depositional environment controls on the geochemistry and oil generation potential of coals and terrigenous kerogens. In: Grimalt, J.O., Dorronsoro, C. (Eds.), Organic Geochemistry: Developments and Applications to Energy, Climate, Environment and Human History, Selected papers from the 17th International Meeting on Organic Geochemistry, pp. 138–141.

Curry, D.J., Emmett, J.K., Hunt, J.W., 1994. Geochemistry of aliphatic-rich coals in the Cooper Basin, Australia and Taranaki basin, New Zealand: implications for the occurrence of potentially oil-generative coals. In: Scott, A.C., Fleet, A.J. (Eds.), Coal and coal-bearing strata as oil-prone source rocks? Geological Society Special Publication No. 77, pp. 149–182.

Cui, N., 2011. Occurrence and exploration for coal beds in Yangxia coal mines, Luntai County, Xinjiang. Western Resources 4, 66–68 (in Chinese).

Dieckmann, V., 2005. Modelling petroleum formation from heterogeneous source rocks: the influence of frequency factors on activation energy distribution and geological prediction. Marine and Petroleum Geology 22, 375–390.

Dieckmann, V., Schenk, H.J., Horsfield, B., Welte, D.H., 1998. Kinetics of petroleum generation and cracking by programmed-temperature closed-system pyrolysis of Toarcian Shales. Fuel 77, 23–31.

Dieckmann, V., Ondrak, R., Cramer, B., Horsfield, B., 2006. Deep basin gas: new insights from kinetic modeling and isotopic fractionation in deep-formed gas precursors. Marine and Petroleum Geology 23, 183–199.

Dieckmann, V., Schenk, H.J., Horsfield, B., 2000. Assessing the overlap of primary and secondary reactions by closed- versus open-system pyrolysis of marine kerogens. Journal of Analytical and Applied Pyrolysis 56, 33–46.

Erdmann, M., Horsfield, B., 2006. Enhanced late gas generation potential of petroleum source rocks via recombination reactions: evidence from the Norwegian North Sea. Geochimica et Cosmochimica Acta 70, 3943–3956.

Espitalié, J., Laporte, J.L., Madec, M., Marquis, F., Leplat, P., Paulet, J., Boutefeu, A., 1977. Méthode rapide de caractérisation des roches mères de leur potentiel pétrolier et de leur degree d'évolution. Revue de l'Institut Francais du Pétrole 32, 23–42.

Espitalié, J., Ungerer, P., Irwin, I., Marquis, F., 1988. Primary cracking of kerogens: Experimenting and modelling C_1, C_2–C_5, C_6–C_{15} and C_{15+} classes of hydrocarbons formed. Organic Geochemistry 13, 893–899.

Graham, S.A., Hendrix, M.S., Wang, L.B., Homewood, P., 1993. Collision successor basins of western China, impact of tectonic inheritance on sand composition. Geological Society of America Bulletin 105, 323–344.

Greensfelder, B.S., Voge, H.H., Good, G.M., 1949. Catalytic and thermal cracking of pure hydrocarbons. Industrial and Engineering Chemistry 41, 2573–2584.

Guo, X., Liu, K., Jia, C., Song, Y., Zhao, M., Zhuo, Q., Lu, X., 2016. Hydrocarbon accumulation processes in the Dabei tight-gas reservoirs, Kuqa Subbasin, Tarim Basin, northwest China. American Association of Petroleum Geologists Bulletin 100, 1501–1521.

Hunt, J.M., 1991. Generation of gas and oil from coal and other terrestrial organic matter. Organic Geochemistry 17, 673–680.

Hill, R.J., Zhang, E., Katz, B.J., Tang, Y., 2007. Modeling of gas generation from the Barnett Shale, Fort Worth Basin, Texas. American Association of Petroleum Geologists Bulletin 91, 501–521.

Horsfield, B., 1989. Practical criteria for classifying kerogens: some observations from pyrolysis-gas chromatography. Geochimica et Cosmochimica Acta 53, 891–901.

Isaksen, G.H., Curry, D.J., Yeakel, J.D., Jenssen, A.I., 1998. Controls on the oil and gas potential of humic coals. Organic Geochemistry 29, 22–44.

Jia, C., Wei, G., Yang, H., Li, L., 1995. Tectonic Evolution and Regional Structural Characteristics in the Tarim Basin. Petroleum Industry Press, Beijing (in Chinese).

Jia, C., He, D., Lei, Z., Zhou, L., Jia, J., Wang, G., 2000. Oil and Gas Exploration in the Foreland Thrust Belt. Petroleum Industry Press, Beijing (in Chinese).

Jia, C., Gu, J., Zhang, G., 2002. Geological constraints of giant and medium-sized gas fields in the Kuqa Depression. Chinese Science Bulletin 47 (Supplementary), 47–54.

Jia, C.Z., Li, Q.M., 2008. Petroleum geology of Kela-2, the most productive gas field in China. Marine and Petroleum Geology 25, 335–343.

Jin, X., Li, E., Pan, C., Yu, S., Liu, J., 2013. Interaction of coal and oil in confined pyrolysis experiments: Insight from the yield and composition of gas hydrocarbons. Marine and Petroleum Geology 48, 379–391.

Katz, B.J., Kelley, P.A., Royle, R.A., Jorjorian, T., 1991. Hydrocarbon products of coals as revealed by pyrolysis-gas chromatography. Organic Geochemistry 17, 711–722.

Killops, S.D., Funnell, R.H., Suggate, R.P., Sykes, R., Peters, K.E., Walters, C.C., Woolhouse, A.D., Weston, R.J., Boudou, J.P., 1998. Predicting generation and expulsion of paraffinic oil from vitrinite-rich coals. Organic Geochemistry 29, 1–21.

Killops, S., Jarvie, D., Sykes, R., Funnell, R., 2002. Maturity-related variation in the bulk-transformation kinetics of a suite of compositionally related New Zealand coals. Marine and Petroleum Geology 19, 1151–1168.

Larter, S.R., Horsfield, B., Douglas, A.G., 1977. Pyrolysis as a possible means of determining the petroleum-generating potential of sedimentary organic matter. In: Jones, C.E.R., Cramers, C.A. (Eds.), Analytical Pyrolysis. Elsevier, Amsterdam, pp. 189–202.

Lei, G., Xie, H., Zhang, J., Wang, Y., Huang, S., Ye, M., Zhang, G., 2007. Structural features and natural gas exploration in the Kelasu structural belt, Kuqa Depression. Oil and Gas Geology 28, 816–820 (in Chinese).

Leif, R.N., Simoneit, B.R.T., 2000. The role of alkenes produced during hydrous pyrolysis of a shale. Organic Geochemistry 31, 1189–1208.

Li, E., Pan, C., Yu, S., Jin, X., Liu, J., 2013. Hydrocarbon generation from coal, extracted coal and bitumen rich coal in confined pyrolysis experiments. Organic Geochemistry 64, 58–75.

Li, E., Pan, C., Yu, S., Jin, X., Liu, J., 2016. Interaction of coal and oil in confined pyrolysis experiments: Insight from the yields and carbon isotopes of gas and liquid hydrocarbons. Marine and Petroleum Geology 69, 13–37.

Liang, D., Zhang, S., Chen, J., Wang, F., Wang, P., 2003. Organic geochemistry of oil and gas in the Kuqa depression, Tarim Basin, NW China. Organic Geochemistry 34, 873–888.
Mansuy, L., Landais, P., Ruau, O., 1995. Importance of the reacting medium in artificial maturation of a coal by confined pyrolysis. 1. Hydrocarbons and polar compounds. Energy & Fuels 9, 691–703.
Mansuy, L., Landais, P., 1995. Importance of the reacting medium in artificial maturation of a coal by confined pyrolysis. 2. Water and polar compounds. Energy & Fuels, 809–821.
McNeil, R.I., BeMent, W.O., 1996. Thermal stability of hydrocarbons: Laboratory criteria. Energy & Fuels 10, 60–67.
Michels, R., Landais, P., Torkelson, B.E., Philp, R.P., 1995. Effects of effluents and water pressure on oil generation during confined pyrolysis and high-pressure hydrous pyrolysis. Geochimica et Cosmochimica Acta 59, 1589–1604.
Michels, R., Burkle, V., Mansuy, L., Langlois, E., Ruau, O., Landais, P., 2000. Role of polar compounds as source of hydrocarbons and reactive medium during the artificial maturation of Mahakam coal. Energy & Fuels 14, 1059–1071.
Monthioux, M., Landais, P., Monin, J.C., 1985. Comparison between natural and artificial maturation series of humic coals from the Mahakam Delta, Indonesia. Organic Geochemistry 8, 275–292.
Monthioux, M., Landais, P., Durand, B., 1986. Comparison between extracts from natural and artificial maturation series of Mahakam Delta coals. Organic Geochemistry 10, 299–311.
Pan, C., Yu, L., Liu, J., Fu, J., 2006. Chemical and carbon isotopic fractionations of gaseous hydrocarbons during abiogenic oxidation. Earth and Planetary Science Letters 246, 70–89.
Pan, C., Geng, A., Zhong, N., Liu, J., Yu, L., 2008. Kerogen pyrolysis in the presence and absence of water and minerals: 1 Gas components. Energy & Fuels 22, 416–427.
Pan, C., Geng, A., Zhong, N., Liu, J., Yu, L., 2009. Kerogen pyrolysis in the presence and absence of water and minerals: amounts and compositions of bitumen and liquid hydrocarbons. Fuel 88, 909–919.
Pan, C., Jiang, L., Liu, J., Zhang, S., Zhu, G., 2010. The effects of calcite and montmorillonite on oil cracking in confined pyrolysis experiments. Organic Geochemistry 41, 611–626.
Pan, C., Jiang, L., Liu, J., Zhang, S., Zhu, G., 2012. The effects of pyrobitumen on oil cracking in confined pyrolysis experiments. Organic Geochemistry 45, 29–47.
Pepper, A.S., 1992. Estimating of petroleum expulsion behavior of source rocks: a novel quantitative approach. In: England, A.J., Fleet, A.J. (Eds.), Petroleum Migration, vol. 59. Geological Society Special Publication, pp. 9–31.
Pepper, A.S., Corvi, P.J., 1995a. Simple kinetic models of petroleum formation. Part I: oil and gas generation from kerogen. Marine and Petroleum Geology 12, 291–319.
Pepper, A.S., Corvi, P.J., 1995b. Simple kinetic models of petroleum formation. Part III: modelling an open system. Marine and Petroleum Geology 12, 417–452.
Pepper, A.S., Dodd, T.A., 1995. Simple kinetic models of petroleum formation. Part II: oil–gas cracking. Marine and Petroleum Geology 12, 321–340.
Peters, K.E., 1986. Guidelines for evaluating petroleum source rock using programmed pyrolysis. American Association of Petroleum Geologists Bulletin 70, 318–329.
Peters, K.E., Walters, C.C., Mankiewicz, P.J., 2006. Evaluation of kinetic uncertainty in numerical models of petroleum generation. American Association of Petroleum Geologists Bulletin 90, 387–403.
Peters, K.E., Burnham, A.K., Walters, C.C., 2015. Petroleum generation kinetics: Single- versus multiple heating-ramp open-system pyrolysis. American Association of Petroleum Geologists Bulletin 99, 591–616.
Powell, T.G., Boreham, C.J., 1991. Petroleum generation and source rock assessment in terrigenous sequences: an update. Australian Petroleum Exploration Association Journal 31, 297–311.
Price, L.C., Wenger, L.M., 1992. The influence of pressure on petroleum generation and maturation as suggested by aqueous pyrolysis. Organic Geochemistry 19, 141–159.
Sandvik, E.I., Young, W.A., Curry, D.J., 1992. Expulsion from hydrocarbon sources: The role of organic absorption. Organic Geochemistry 19, 77–87.
Schenk, H.J., Horsfield, B., 1993. Kinetics of petroleum generation by programmed-temperature closed- versus open-system pyrolysis. Geochimica et Cosmochimica Acta 57, 623–630.
Schenk, H.J., di Primo, R., Horsfield, B., 1997. The conversion of oil into gas in petroleum reservoirs. Part 1: Comparative kinetic investigation of gas generation from crude oils of lacustrine, marine and fluviodeltaic origin by programmed temperature closed-system pyrolysis. Organic Geochemistry 26, 467–481.
Smith, J.W., Gilbert, T.D., Batts, B.D., 1987. A quest for a new parameter in petroleum exploration geochemistry. Australian Petroleum Exploration Association Journal 27, 98–105.
Smith, J.W., Batts, B.D., Gilbert, T.D., 1989. Hydrous pyrolysis of model compounds. Organic Geochemistry 14, 365–373.
Sweeney, J.J., Burnham, A.K., 1990. Evaluation of a simple model of vitrinite reflectance based on chemical kinetics. American Association of Petroleum Geologists Bulletin 74, 1559–1570.
Sykes, R., Snowdon, L.R., 2002. Guidelines for assessing the petroleum potential of coaly source rocks using Rock-Eval pyrolysis. Organic Geochemistry 33, 1441–1455.
Tang, Y., Jenden, P.D., Nigrini, A., Teerman, S.C., 1996. Modeling early methane generation in coal. Energy & Fuels 10, 659–671.
Tegelaar, E.W., Noble, R.A., 1994. Kinetics of hydrocarbon generation as a function of the molecular structure of kerogen as revealed by pyrolysis–gas chromatography. Organic Geochemistry 22, 543–574.
Ungerer, P., Pelet, R., 1987. Extrapolation of the kinetics of oil and gas formation from laboratory experiments to sedimentary basins. Nature 327, 52–54.
Van Krevelen, D.W., 1961. Coal. Elsevier, Amsterdam.
Wang, Z., 2014. Formation mechanism and enrichment regularities of Kelasu subsalt deep large gas field in Kuqa Depression, Tarim Basin. Natural Gas Geoscience 25 (2), 153–166 (in Chinese).
Wang, Z., Xie, H., Li, Y., Lei, G., Wu, C., Yang, X., Ma, Y., Neng, Y., 2013. Exploration and discovery of large and deep subsalt gas fields in Kuqa Foreland Thrust Belt. China Petroleum Exploration 18 (3), 1–11 (in Chinese).
Xiang, B., Li, E., Gao, X., Wang, M., Wang, Y., Xu, H., Huang, P., Yu, S., Liu, J., Zou, Y., Pan, C., 2016. Petroleum generation kinetics for Permian lacustrine source rocks in the Junggar Basin, NW China. Organic Geochemistry 77, 1–17.
Xu, H., Ding, X., Luo, Z., Liu, C., Li, E., Huang, P., Yu, S., Liu, J., Zou, Y., Pan, C., 2017. Confined pyrolysis for simulating hydrocarbon generation from Jurassic coaly source rocks in the Junggar Basin, Northwest China. Energy & Fuels 31, 73–94.
Yang, X., Gu, J., Jia, J., Zhang, B., 2005. Sedimentary development and infill pattern of the Mesozoic and Cenozoic foreland basins in central and western China. Natural Gas Exploration and Development 28 (1), 1–4 (in Chinese).
Yu, Y., Muhtarzari, Wu, M., 2013. Geological structure and coal petrographic characteristics of Luntai Weidong Mine. Xinjiang: Journal of Jixi University 13 (9), 54–56 (in Chinese).
Zhang, S., Zhang, B., Zhu, G., Wang, H., Li, Z., 2011. Geochemical evidence for coal-derived hydrocarbons and their charge history in the Dabei Gas Field, Kuqa Thrust Belt, Tarim Basin, NW China. Marine and Petroleum Geology 28, 1364–1375.
Zhao, W., Zhang, S., Wang, F., Cramer, B., Chen, J., Sun, Y., Zhang, B., Zhao, M., 2005. Gas systems in the Kuche Depression of the Tarim Basin: source rock distributions, generation kinetics and gas accumulation history. Organic Geochemistry 36, 1583–1601.
Zieger, L., Littke, R., Schwarzbauer, J., 2018. Chemical and structural changes in vitrinites and megaspores from Carboniferous coals during maturation. International Journal of Coal Geology 185, 91–102.